

1 Comparative genomics reveals the origin of fungal 2 hyphae and multicellularity

3
4 Enikő Kiss^{1,2}, Botond Hegedüs¹, Torda Varga¹, Zsolt Merényi¹, Tamás Kószó¹, Balázs
5 Bálint¹, Arun N. Prasanna^{1&}, Krisztina Krizsán¹, Meritxell Riquelme³, Norio Takeshita⁴,
6 László G. Nagy^{1*}

7
8
9 ¹Synthetic and Systems Biology Unit, Institute of Biochemistry, BRC-HAS, 6726 Szeged,
10 Hungary

11 ²University of Szeged, Faculty of Science and Informatics, 6720, Szeged, Hungary

12 ³Department of Microbiology, Centro de Investigación Científica y de Educación Superior de
13 Ensenada, 22860 Ensenada, Baja California, Mexico

14 ⁴Microbiology Research Center for Sustainability (MiCS), Faculty of Life and Environmental
15 Sciences, University of Tsukuba, 305-8572, Japan

16
17 *Author for correspondence: lnagy@fun genomelab.com

18 &Current address: Red Sea Science and Engineering Research Center, 4700 King Abdullah
19 University of Science and Technology (KAUST), Thuwal 23955-6900, Kingdom of Saudi Arabia

22 Abstract

23 Hyphae represent a hallmark structure of multicellular fungi with immense importance in their
24 life cycle, including foraging for nutrients, reproduction, or virulence. Hypha morphogenesis has
25 been the subject to intense interest, yet, the origins and genetic underpinning of the evolution of
26 hyphae are hardly known. Using comparative genomics, we here show that the emergence of
27 hyphae correlates with multiple types of genetic changes, including alterations of gene structure,
28 gene family diversification as well as co-option and exaptation of ancient eukaryotic genes (e.g.
29 phagocytosis-related genes). Half of the gene families involved in hypha morphogenesis have
30 homologs in unicellular fungi and non-fungal eukaryotes and show little or no duplications
31 coincident with the origin of multicellular hyphae. Considerable gene family diversification was
32 observed only in transcriptional regulators and genes related to cell wall synthesis and
33 modification. Despite losing 35-46% of their genes, yeasts retained significantly more
34 multicellularity-related genes than expected by chance. We identified 414 gene families that
35 evolved in a correlated fashion with hyphal multicellularity and may have contributed to its
36 evolution. Contrary to most multicellular lineages, the origin of hyphae did not correlate with the
37 expansion of gene families encoding kinases, receptors or adhesive proteins. Our analyses
38 suggest that fungi took a unique route to multicellularity that involved limited gene family
39 diversification and extensive co-option of ancient eukaryotic genes.

40 Introduction

41 The evolution of multicellularity (MC) is considered one of the major transitions in the history of
42 life¹. It evolved in several pro- and eukaryote lineages²⁻⁷, each representing a unique solution to
43 the challenges of multicellular organization⁶. Among the eukaryotes, two major modes for
44 acquiring multicellularity are the clonal and aggregative routes^{5,6,8-10}, which differ in how multi-
45 celled precursors emerged by adhesion, cooperation, communication and functional
46 diversification of cells^{3,11,12}.

47
48 Fungi represent one of the three kingdoms where multicellular forms dominate among
49 extant species¹³, yet, our knowledge on the evolutionary origin of multicellularity in this group is
50 very incomplete. While most multicellular lineages can be recognized as either clonal or
51 aggregative by comparisons to their unicellular relatives, fungal multicellularity has been
52 recalcitrant to such categorization^{6,14}. The thalli of fungi are made up of hyphae, thin, tubular
53 structures that grow by apical extension to form a mycelium that explores and invades the
54 substrate. Hyphal multicellularity has a number of unique properties compared to clonal and
55 aggregative multicellularity, raising the possibility that its evolution follows markedly different
56 principles⁷. First, hyphae might have evolved by the gradual elongation of substrate-anchoring
57 rhizoids of early fungi¹⁵⁻¹⁸, through multinucleate intermediates, in contrast to clonal and
58 aggregative lineages, where the first multi-celled clusters probably emerged via related cells
59 sticking together (e.g. choanoflagellates¹⁹), or gathering to form a syncytial body (e.g.
60 *Capsaspora*)⁹. Because early hyphae were uncompartimentarized, their evolution could have
61 bypassed the need to resolve group conflicts and align the fitness of individual cells⁷.
62 Alternatively, it is possible that conflicts are resolved at the level of individual nuclei²⁰. Second,
63 hyphae maximize foraging and nutrient assimilation efficiency and minimize competition for
64 nutrients by a fractal-like growth mode^{16,21,22}. This mode of origin differs from that of other
65 multicellular lineages where selection for increased size possibly helped avoiding predation².
66 Hyphae might have also facilitated the transition of fungi to terrestrial life²³ and confer immense
67 medical relevance to pathogenic fungi²⁴. Hyphae of extant fungi rarely stick to each other in
68 vegetative mycelia and adhesion becomes key only in fruiting bodies²⁵⁻²⁷ - which, in terms of
69 complexity level, resemble complex multicellular metazoans and plants^{7,28} - or in the attachment
70 to host surfaces²⁹. Thus, whereas in most multicellular lineages adhesion, cell-cell cooperation,
71 communication and differentiation represent the main hurdles to the emergence of multicellular
72 precursors^{3,6,30-32}, fungi might have had different obstacles to overcome.

73
74 While the origins of hyphae are poorly known, information on the molecular and cellular
75 basis of hyphal morphogenesis is abundant (for recent reviews see refs³³⁻³⁸), permitting
76 evolutionary genomic analyses of the origins of hyphae. Hyphal morphogenesis builds on cell
77 polarization networks³⁹, the exo- and endocytotic machinery⁴⁰, long range vesicle transport as
78 well as fungal-specific traits such as cell wall synthesis and assembly⁴¹, and the selection of
79 branching points and sites of septation⁴², among others. A key structure of hyphal growth is the
80 Spitzenkörper⁴³, which acts as a distribution center for vesicles transporting cell wall materials
81 and various factors to the hyphal tip. The cytoplasmic microtubule network provides the
82 connection between vesicle cargo through the ER and Golgi and the Spitzenkörper, from where

83 vesicles move along actin microfilaments to the hyphal tip and secrete their content to deposit
84 new cell wall components and provide surface expansion. Further key processes include the
85 recycling of excess membrane in the subapical zone, the activation of cAMP pathways and
86 mitogen activated protein kinase (MAPK) cascades and finally the transcriptional control of
87 morphogenesis (for detailed reviews see refs⁴⁴⁻⁴⁹).

88
89 A complex hyphal thallus has been reported from a 407 million year old fossil
90 Blastocladiomycota⁵¹, whereas Glomeromycotina-like hyphae and spores were preserved 460
91 million years ago^{50,52} indicating that hyphal growth dates back to at least the Ordovician. Most
92 Dikarya and Mucoromycota grow true hyphae, whereas a significant diversity of forms is found
93 in the early diverging Blastocladiomycota, Chytridiomycota and to a smaller extent the
94 Zoopagomycota. The Chytridiomycota is dominated by unicellular forms that anchor themselves
95 to the substrate by branched, root-like rhizoids^{16,50} which have been hypothesized as the
96 precursors to hyphae^{15,53}. An alternative hypothesis designates hypha-like connections in the
97 thalli of polycentric chytrid fungi (e.g. *Physocladia*) as intermediates to true hyphae¹⁷. Like
98 chytrids, most Blastocladiomycota form mono- or polycentric, unicellular thalli, although some
99 species form wide, apically growing structures resembling true hyphae (e.g. *Allomyces*) or
100 narrow exit tubes on zoosporangia (e.g. *Catenaria* spp.)^{16,50,54}. In spite of these intermediate
101 forms, the unicellular dominance in these phyla aligns well with a unicellular ancestry and
102 potential convergent origins of hypha-like structures¹⁷.

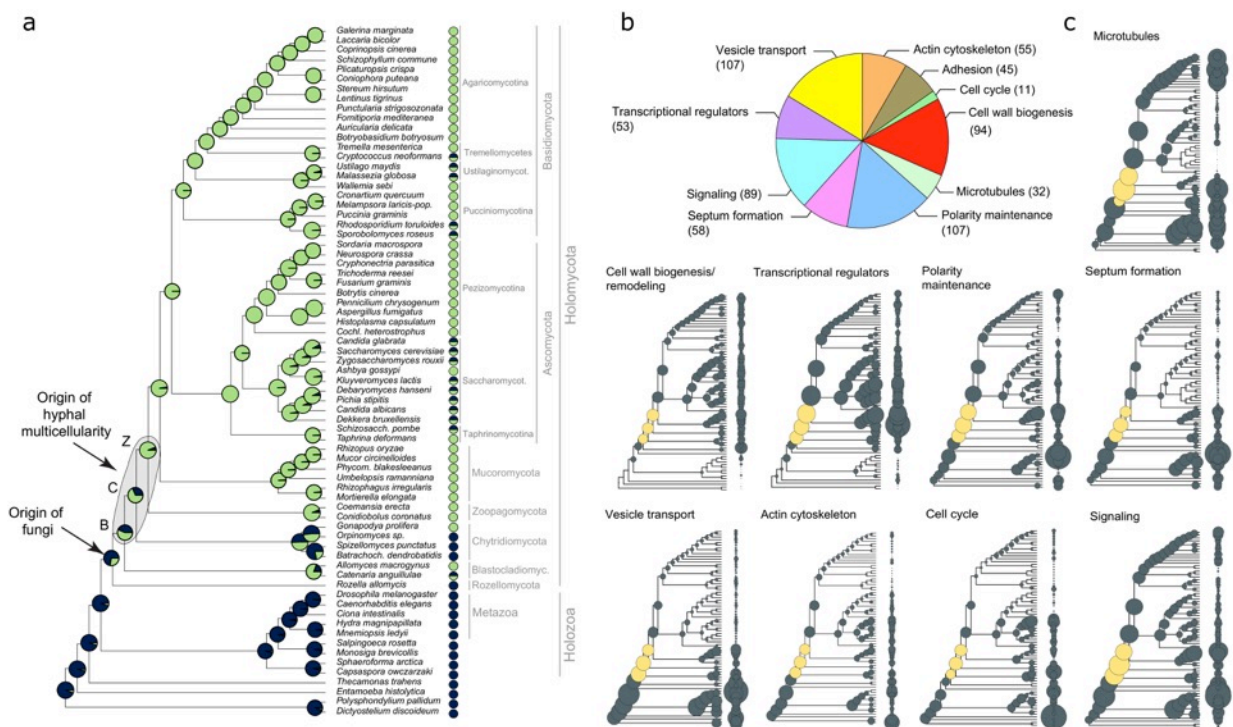
103
104 Here we examine the evolution of hyphal multicellularity in fungi by reconstructing
105 historical patterns of known hyphal morphogenesis genes as well as by systematic searches of
106 fungal genomes for gene families whose evolution correlates with that of hyphae. We analyze
107 the genomes of 4 plesiomorphically unicellular, 40 hyphal (one of which is ambiguous) and 14
108 secondarily simplified (yeast-like) fungi as well as 13 non-fungal relatives. Given the likely
109 convergent origins of hyphae, we focus our analyses on multiple nodes of the fungal tree to
110 where origin(s) of hyphal growth can be localized with confidence. Our analyses reveal a deep
111 eukaryotic origin of most morphogenesis-related families, limited gene family diversification in
112 correlation with the emergence of hyphal MC and that secondarily simplified yeast-like fungi
113 retained most of the genes for multicellular growth.

114 Results and discussion

115 Hyphae evolved in early fungal ancestors

116 To understand the origin of hyphae, we constructed a species phylogeny representing 71
117 species (Supplementary Table 1) by maximum likelihood analysis of a supermatrix of 595
118 single-copy orthologs (175,535 characters Fig. 1a).

119



120
 121 Fig. 1. The evolution of hyphal multicellularity and underlying genes in fungi. (a) Phylogenetic
 122 relationships among 71 species analyzed in this study. Pie charts at nodes show the proportional
 123 likelihoods of hyphal (green) and non-hyphal (dark blue) ancestral states reconstructed using Bayesian
 124 MCMC. Character state coding of extant species used in ancestral state reconstructions is shown next to
 125 species names. BCZ nodes: origin of hyphal growth could be assigned with confidence are highlighted
 126 (note the uncertainty imposed by filamentous Blastocladiomycota). (b) the distribution of literature-
 127 collected hypha morphogenesis genes among 10 main functional categories. (c) Ancestral
 128 reconstructions of gene copy number in 9 main hypha morphogenesis-related categories of genes (see
 129 Fig. 5c for adhesion). Bubble size is proportional to reconstructed ancestral gene copy number. BCZ
 130 nodes are shown in yellow.

131
 132 Our species phylogeny recapitulates recent genome-based phylogenies of fungi^{55–58}, with the
 133 Rozellomycota, Blastocladiomycota and the Chytridiomycota splitting first, second and third off
 134 of the backbone, respectively (ML bootstrap: 100%). We performed ancestral character state
 135 reconstruction using Bayesian MCMC to identify the putative origin of hyphal growth. This
 136 supported an emergence of hyphae from unicellular ancestors in basal fungi. The distribution of
 137 posterior probability values indicated three nodes as the most likely origins of hyphal
 138 multicellularity, which represent the split of Blastocladiomycota, Chytridiomycota and
 139 Zoopagomycota lineages, referred hereafter to as BCZ nodes. The posterior probability for the
 140 hyphal state started to rise in the most recent common ancestor (MRCA) of the
 141 Blastocladiomycota and higher fungi (PP: 0.53, Fig. 1a) and increased to 0.68 and 0.92 in the
 142 next two nodes along the backbone of the tree. This suggests that hyphae evolved either in one
 143 of the BCZ nodes or it may have been a gradual process unfolding in these three nodes. This
 144 uncertainty likely reflects diverse hypha-like morphologies in the Blastocladio- and
 145 Chytridiomycota and is consistent with the convergent origins of hypha-like morphologies^{7,17,18}.

146 To account for this uncertainty, we focus on BCZ nodes in subsequent analyses of hypha
147 morphogenesis genes.

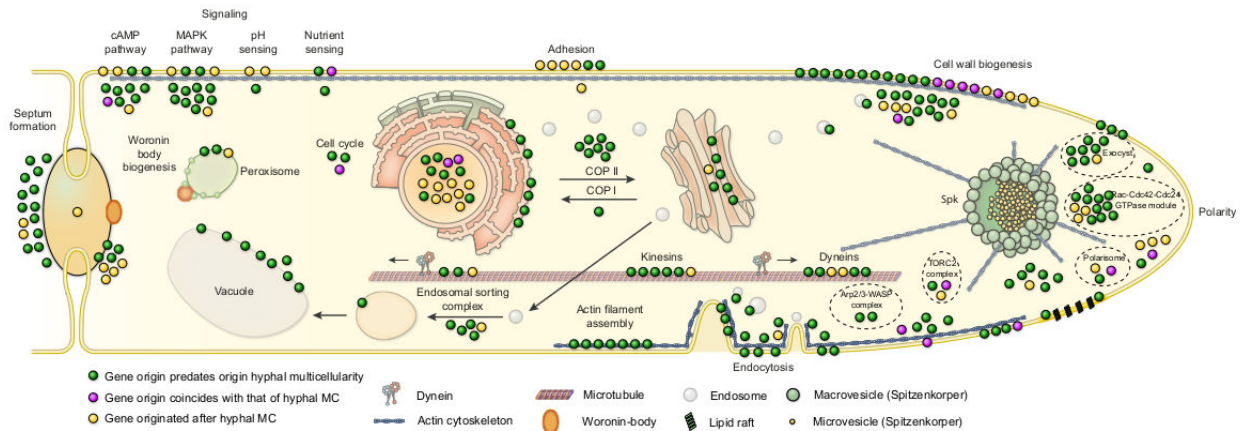
148

149 The evolution of hypha morphogenesis genes

150 Our survey of the literature for hyphal multicellularity-related genes yielded 651 genes (from 519
151 publications), mostly from well-studied model systems such as *A. fumigatus*, *A. nidulans*, *N.*
152 *crassa*, *S. cerevisiae* and *C. albicans* (Supplementary Table 2). We categorized genes
153 according to the broader function they fulfill in hyphal growth into nine functional groups: actin
154 cytoskeleton regulation, polarity maintenance, cell wall biogenesis/remodelling, septation
155 (including septal plugging), signaling, transcriptional regulation, vesicle transport, microtubule-
156 based transport and cell cycle regulation. The categories “polarity maintenance” and “vesicle
157 transport” contained the largest number of genes (107 in each), whereas “cell cycle regulation”
158 contained the fewest (11) (Fig.1b). The collected genes grouped into 362 families by Markov
159 clustering of the a 71-genome dataset.

160

161 Reconstructions of gene duplication/loss histories for nine functional categories of hypha
162 morphogenesis gene families are shown on Fig. 1c. A general pattern that emerges from these
163 is that the origin of many gene families (181 families, 50%) predate that of hyphal MC (Fig. 2,
164 Supplementary Fig. 1), indicating that fungi have co-opted several conserved eukaryotic
165 functionalities for hyphal growth. A significant proportion of multicellularity-related gene families
166 (164 families, 45.3%) emerged after the origin of hyphal MC, indicating lineage- and species-
167 specific genetic innovations. Only 17 families (4.7%) originated in BCZ nodes and were
168 conserved thereafter (Table 1), providing potential candidates that shaped the evolution of
169 hyphal MC. These include two families of transcriptional regulators (encoding StuA and MedA
170 proteins in *A. fumigatus*)^{59,60}, six related to cell wall biogenesis, three to actin cytoskeleton
171 regulation, three to polarity maintenance, two families involved in signaling and one involved in
172 cell cycle regulation. One of the families contains the *S. cerevisiae* Pan1, an endocytic adaptor
173 protein at the plasma membrane. Pan1 triggers the recruitment of the Arp2/3 complex to the site
174 of endocytosis, which is necessary for the recycling of excess membrane in the subapical region
175 during hyphal growth⁴⁰. Another example is the polarisome component BNI-1 from *N. crassa*.
176 Knockout studies showed that it mediates actin cable assembly in filamentous fungi and has a
177 role in diverse morphogenesis-related processes⁶¹. Other proteins involved in establishing cell
178 polarity are the Bem1 actin cytoskeleton reorganizing factor^{62,63} and the Rax1, associated with
179 bipolar budding in *S. cerevisiae*⁶⁴.



180
181 Fig. 2. Phylogenetic age distribution of hypha morphogenesis genes. Schematic outline of terminal hyphal
182 cell is shown with genes marked by dots and colored by phylogenetic age. Genes whose origin predates
183 that of hyphal multicellularity (green, 72,2%) dominate the hyphal morphogenetic machinery, followed by
184 genes that originated after hyphal MC (yellow, 21,2%) and genes whose origin approximately coincides
185 with that of hyphae (purple, 6,6%). Data based on only *A.fumigatus* orthologs. See also Supplementary
186 Figure 1 for gene names.
187

Emergence of gene family	<i>A. fumigatus</i> ortholog	<i>S. cerevisiae</i> ortholog	functional category	cluster ID
	Afu7g03870	PAN1/YIR006C	actin cytoskeleton	4903
	crh3/Afu3g09250	UTR2/YEL040W	cell wall biogenesis	374
Ica of Dikarya, Mucoromycota, Zoopagomycota, Chytridiomycota, Blastocladiomycota	gel7/Afu6g12410	GAS1/YMR307W	cell wall biogenesis	435
	Afu6g04940	BNR1/YIL159W	polarity establishment	3689
	Afu4g04120	BEM1/YBR200W	polarity establishment	2482
	stuA/Afu2g07900	PHD1/YKL043W	transcriptional regulation	2479
	medA/Afu2g13260	NA	transcriptional regulation	8521
	Afu6g07910	SLM1/YIL105C	actin cytoskeleton	1561
	Afu8g04520	SLA1/YBL007C	actin cytoskeleton	5953
	Afu4g06130	WHI2/YOR043W	cell cycle regulation	2915
Ica of Dikarya, Mucoromycota, Zoopagomycota, Chytridiomycota	Afu4g00620	DFG5/YMR238W	cell wall biogenesis	843
	Afu8g02320	NA	cell wall biogenesis	3398
	chsD/Afu1g12600	NA	cell wall biogenesis	9065
	rgsB/Afu4g12640	RAX1/YOR301W	polarity establishment	2900
	Afu2g08800	SSY1/YDR160W	signaling	49
	ricA/Afu4g08820	NA	signaling	5950
Ica of Dikarya, Mucoromycota, Zoopagomycota	kre6/Afu2g11870	KRE6/YPR159W	cell wall biogenesis	293

188 Table 1: List of the 17 gene families whose emergence shows correlation with the evolution of hyphal MC
189 based on COMPARE analysis.
190

191 Gene families related to septation, polarity maintenance, cell cycle control, vesicle
192 transport and microtubule-based transport are generally more diverse in animals, non-fungal
193 eukaryotes and their ancestors than in fungi, suggesting that despite the key role of these

194 families in hyphal MC, they evolved primarily by gene loss in fungi (Fig 1c). Cell wall synthesis
195 and remodeling as well as transcription regulation related families, on the other hand, show
196 expansions in MC fungi, suggesting that the diversification of these gene families could have
197 played roles in the evolution of hyphal MC (Fig 1c).

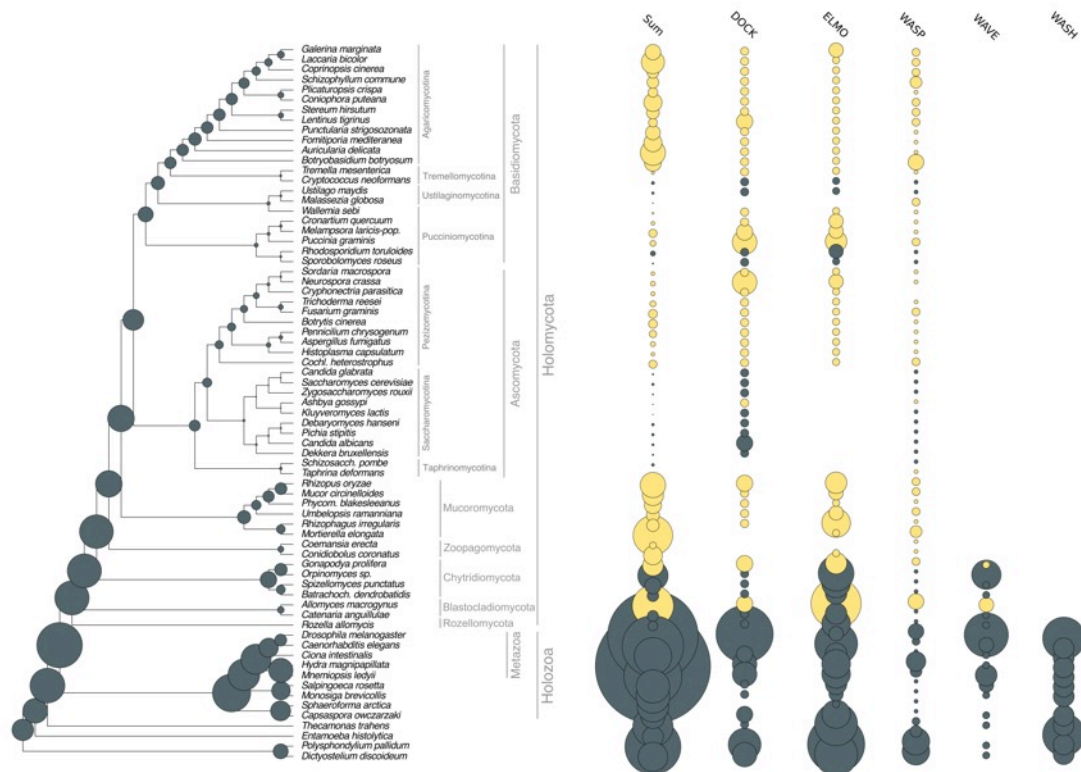
198
199 Ninety-three (25.7%) of the 362 hyphal morphogenesis-related gene families showed
200 duplications in BCZ nodes (Supplementary Table 3). Enrichment analysis of gene duplications
201 revealed no individual gene families with significantly increased number of duplications
202 (Benjamini-Hochberg corrected $P < 0.05$, Fisher's exact test) in BCZ nodes, relative to the rest of
203 the tree (Supplementary Table 4). The same analysis on the 9 functional groups showed
204 significantly increased numbers of duplications in the cell wall biogenesis and transcriptional
205 regulation categories. These analyses suggest that the evolution of hyphal growth in BCZ nodes
206 did not generally coincide with a period of extensive gene duplication except in cell wall
207 biogenesis and transcriptional regulation-related gene families. Collectively, reconstructions of
208 gene family evolution revealed the lack of a major burst of gene family origin or that of
209 duplications coincident with the evolution of hyphal MC.

210
211 We analyzed whether changes in basic structural properties of genes show a correlation
212 with the evolution of hyphal MC. Significant differences ($P < 0.05$) were observed in gene, CDS
213 and intron lengths between unicellular and multicellular fungi (Supplementary Fig. 2,
214 Supplementary Table 5). CDS lengths of septation and polarity maintenance genes were
215 significantly higher in multicellular than in unicellular fungi ($P=0.0012-0.00017$, Supplementary
216 Fig. 2). An opposite pattern was observed in intron lengths, which were on average longer in
217 unicellular fungi in actin cytoskeleton, cell wall biogenesis, polarity maintenance, septation and
218 vesicle transport related genes. In actin cytoskeleton-related genes the CDS length and intron
219 length showed the same pattern: both of them were longer in multicellular species. Gene and
220 CDS lengths were significantly longer in unicellular than in multicellular fungi in genes encoding
221 adhesion and microtubule-based transport proteins. On the other hand, interestingly, no
222 significant changes in gene structure were detected in cell wall biogenesis and transcriptional
223 regulation-related genes, the two categories that displayed significant gene family diversification
224 in early filamentous fungi.

225 Phagocytosis is lost, but phagocytotic genes are retained by fungi

226 Our sets of hypha morphogenesis genes included several entries associated with phagocytosis
227 in non-fungal eukaryotes. This is surprising given that phagocytosis is not known in fungi and
228 their rigid cell wall forms a physical barrier to it. We therefore examined the fate of phagocytosis
229 genes in filamentous fungi based on the phagocytotic machinery of *D. discoideum*^{65,66} and other
230 eukaryotes⁶⁷. Filamentous fungi have retained several phagocytotic gene families but lost others
231 (Fig. 3). For example, members of the Arp2/3 complex, which nucleates actin filaments and
232 triggers actin cytoskeleton rearrangements⁶⁸ is conserved in filamentous fungi and is involved in
233 hyphal growth⁶⁹. Engulfment and cell motility genes (ELMO1/2) are found in all filamentous
234 fungi, but are convergently lost in budding and fission yeasts as well as in *C. neoformans*, *M.*
235 *globosa* and *W. sebi*, all of which have reduced capacities for hyphal growth. The DOCK
236 (dedicator of cytokinesis) protein family, which interacts with ELMO proteins, is represented as a

237 single gene copy in filamentous fungi and yeasts. This family contains orthologs of *S. cerevisiae*
 238 DCK1 (a homolog of human DOCK1), which has been shown to influence hypha
 239 morphogenesis⁷⁰. Of the broader Wiskott-Aldrich syndrome family of proteins, which reorganize
 240 the actin cytoskeleton during phagocytosis, the WASP family is conserved across fungi, the
 241 WAVE family is only represented in early diverging fungi and non-fungal eukaryotes, whereas
 242 the WASH family has been lost in fungi, with homologs detected only in non-fungal eukaryotes,
 243 consistent with recent reports^{71,72}. These patterns reveal the conservation of several
 244 phagocytotic genes in fungi, despite the loss of phagocytosis and the evolution of rigid cell walls
 245 and osmotrophy. Previous functional analyses have shown that several of the retained genes
 246 are involved in hypha morphogenesis in fungi, indicating that members of the phagocytic
 247 machinery were probably exapted for hyphal multicellularity in ancient fungi.



248
 249 Fig. 3. Evolutionary dynamics of phagocytosis-related gene families. Several phagocytic gene families
 250 retained in filamentous fungi (DOCK, ELMO, WASP). WAVE family retained only in early fungi
 251 (Blastocladiomycota and Chytridiomycota), WASH family is represented only in non-fungal eukaryotes.
 252 Bubble size is proportional to ancestral and extant gene copy number. Copy numbers of filamentous fungi
 253 are labelled with yellow.
 254

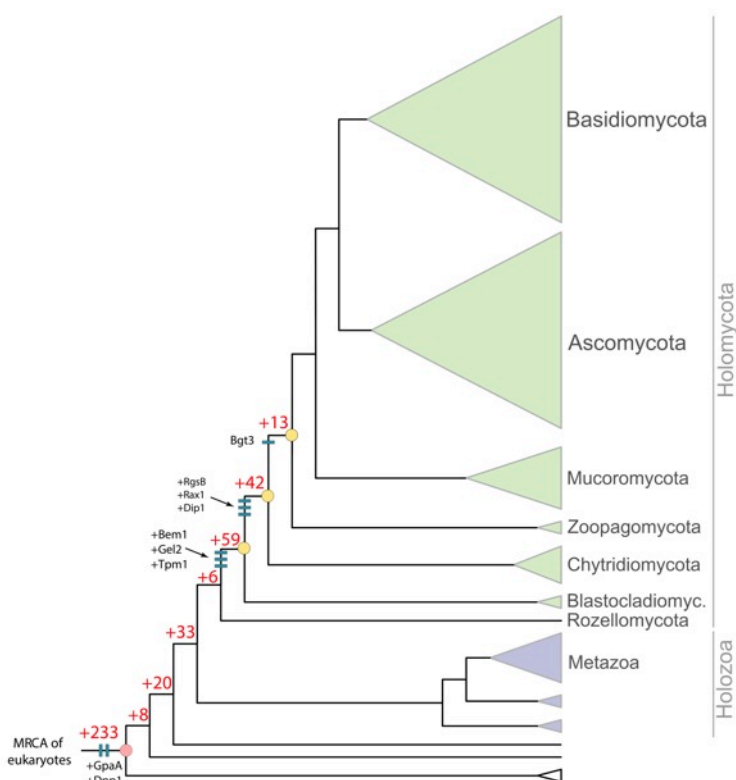
255 Genome-wide screen for correlated evolution between multicellularity and 256 gene family expansion

257 To identify further gene families with a potential connection to hyphal MC, we systematically
 258 searched for families that show substantial dynamics in BCZ nodes. We reasoned that gene
 259 families underlying hyphal MC should originate or diversify in BCZ nodes and be conserved in

260 descendent filamentous fungi. Searching for gene families fitting these criteria yielded 414
261 families (ANOVA, $p < 0.05$, Supplementary Table 6), 114 of which originated in BCZ nodes, while
262 the others showed duplication rates that exceeded the expectation derived from genome-wide
263 collection of gene families (Fig. 4). These included several known morphogenetic families (e.g.
264 Bgt3, RgsB and Gel2 of *A. fumigatus*, Bem1 and Rax1 of *S. cerevisiae*), genes involved in actin
265 cytoskeleton and cell wall assembly, mating, pheromone response (GpaA of *A. fumigatus*),
266 sporulation and transporters, among others (Supplementary Table 6). Several of the identified
267 families contain genes with reported growth defects in *A. fumigatus* or *S. cerevisiae*, indicating
268 that our searches recovered genes relevant for hyphal MC. For example, Rax proteins are
269 major regulators of cellular morphogenesis and are involved in bud site selection in budding
270 yeasts^{73,74}, polarized growth in *S. pombe*⁷⁵ and polarity maintenance in filamentous fungi⁷⁶. The
271 finding that these families originated in BCZ nodes makes them candidates for being key
272 contributors to the evolution of hyphal MC. We further detected a fungal-specific cluster of
273 tropomyosins (TPM1 in *S. cerevisiae*), which maps to the MRCA of Blastocladiomycota and
274 other fungi and comprises genes involved in polarized growth and the stabilization of actin
275 microfilaments. The family containing *S. pombe* Dip1 homologs (Afu6g12370 in *A. fumigatus*)
276 emerged in the node uniting Chytridiomycota with higher fungi and contains a single gene per
277 species afterwards, except an expansion in WGD Mucoromycota⁷⁷ and losses in the
278 Saccharomycotina. In *S. pombe*, Dip1 activates the Arp2/3 complex without preexisting actin
279 cables^{78,79} and thus initiates cortical actin patch assembly and endocytosis. Because it does not
280 require pre-existing actin cables, it mediates actin cytoskeleton regulation through a mechanism
281 that seems to be specific to multicellular fungi. Finally, we detected the family containing *S.*
282 *cerevisiae* Dpp1 homologs, which shows a significant expansion (4 duplications) in BCZ nodes.
283 This family regulates morphogenetic transitions in dimorphic fungi through the synthesis of the
284 fungal signal molecule farnesol⁸⁰, which prompts us to speculate that it might have contributed
285 to the elaboration of farnesol-based communication in fungi.

286
287 Because the emergence of hyphal multicellularity overlaps significantly with that of other
288 fungal traits, it is challenging to unequivocally separate signals conferred by these traits from
289 those of hyphal MC. It is conceivable that a portion of the 414 gene families (Supplementary
290 Table 6) were detected because of signals conferred by phylogenetically co-distributed traits,
291 not necessarily multicellularity itself (see Beaulieu 2016⁸¹ for a conceptually analogous problem
292 in analyzing taxonomic diversification). One such trait could be osmotrophy, the feeding
293 mechanism of fungi to absorb soluble goods generated by extracellular enzyme complexes⁸².
294 We detected 20 gene families that showed strong correlation with hyphal MC and were
295 annotated as various transporters; such families could hypothetically be related to osmotrophy.
296 Further, among the 414 detected families, there were 84 that are currently functionally
297 uncharacterized and thus it is impossible to speculate about their role in hyphal MC.
298 Collectively, these families indicate that there are plenty of fungal genes that evolved in concert
299 with hyphal MC and that await functional characterization to establish links to hyphal MC or
300 other fungal functions.

301



302
 303 Fig. 4. Origin of 414 gene families potentially related to the evolution of hyphal MC, identified by ANOVA
 304 ($p < 0.05$). 114 families originated in BCZ nodes, including known morphogenesis related proteins (e.g.
 305 Bgt3, RgsB, Gel2 of *A. fumigatus*, Rax1, Bem1, Tpm1 and Dpp1 from *S. cerevisiae*, Dip1 from *S. pombe*)
 306 labelled as blue bars. Red numbers at branches represent the number of gene families originated at the
 307 backbone of the species tree.

308 The evolution of kinase, receptor and adhesive repertoires do not correlate 309 with hyphal multicellularity

310 The increased sophistication of cell-cell communication and adhesion pathways often correlates
 311 with expanded repertoires of genes encoding kinases, receptors and adhesive proteins^{83–85}. We
 312 therefore, examined Ser/Thr kinase (954 clusters), hybrid histidine kinase (96 clusters), receptor
 313 (183 clusters) and adhesion (23 clusters) genes, focusing on the comparison of unicellular and
 314 filamentous fungi. Copy numbers across the 954 identified Ser/Thr kinase clusters were similar
 315 in unicellular and simple multicellular fungi, with higher kinase diversity found in complex
 316 multicellular Basidiomycota (as reported by Krizsan 2018)⁸⁶ and in *Rhizophagus irregularis* (Fig.
 317 5a). We inferred net contractions in BCZ nodes, from 572 to 529 reconstructed ancestral
 318 kinases (81 duplications, 124 losses, Fig. 5a). Nevertheless, kinase families that duplicated here
 319 include all 3 MAPK pathways in fungi, the mating pheromone, cell wall integrity (*fus3*, *kss1*,
 320 *kdx1* from *S. cerevisiae*, *mpkB* from *A. fumigatus*) and osmoregulatory pathways (*hog1*, *ssk2*,
 321 *ssk22* from *S. cerevisiae*, *sakA*, *sskB* from *A. fumigatus*), all of which indirectly regulate hyphal
 322 growth^{46–48}.

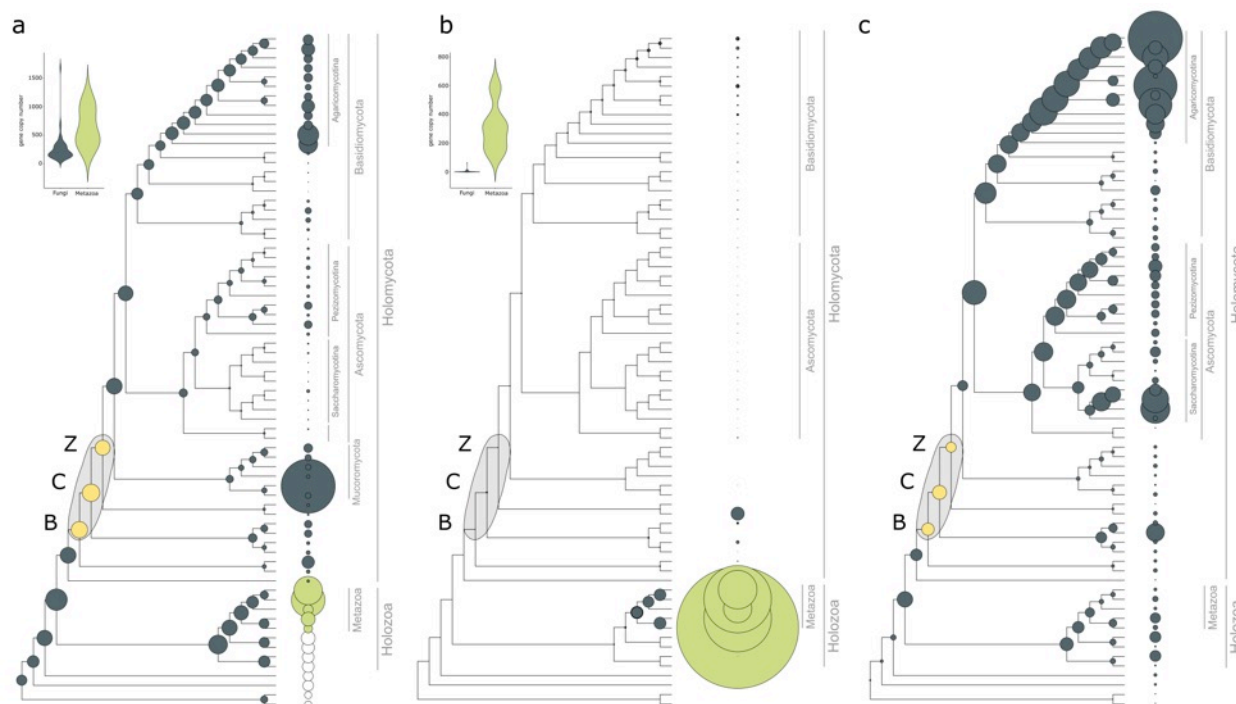
323 Overall, fungi had fewer Ser/Thr kinases (mean 257) than metazoans (mean 643).
 324 However, the higher kinase diversity of metazoans seems to be a result of an early expansion in

325 the MRCA of Holomycota and Holozoa (Fig. 5a). While signal transduction requirements of
326 metazoan MC have been mostly discussed in the context of receptor tyrosine kinases, we found
327 no evidence for domain architectures typical of receptor tyrosine kinases in fungi. The only
328 group resembling receptor kinases is hybrid histidine kinases (HK), that comprise proteins with
329 a sensor domain, a histidine kinase domain and a C-terminal receiver domain that acts as a
330 response regulator. We inferred an expansion (24 duplications, 10 losses) of HKs in the MRCA
331 of the Chytridiomycota and other fungi, including class III and X HKs, which are linked to
332 morphogenesis^{87,88}. Another wave of HK expansion was inferred in the MRCA of Mucoromycota
333 and Dikarya with 11 duplications and 4 losses (Supplementary Fig. 3).

334
335 In G-protein coupled receptors (GPCRs), an even more extreme difference was
336 observed between fungi and metazoans (Fig. 5b). A large receptor expansion was observed in
337 the latter, which resulted in 135-583 genes in extant animals. Out of the 183 analyzed GPCR
338 families, only 19 were found in fungi, and only one of them was generally conserved across
339 fungal species. This family contains STE3 and STE3-like α -factor mating pheromone receptors,
340 involved in pheromone-dependent signal transduction, cellular conjugation and cell fusion.

341
342 Adhesive cell surface proteins are key mediators of the transition to MC in colonial and
343 aggregative lineages^{3,5,6}, which is reflected in their higher copy numbers in multicellular
344 organisms⁸⁹. We identified 45 families of putative adhesion-related proteins in fungi, including
345 adhesins, flocculins, hydrophobins, various lectins and glycosylphosphatidylinositol (GPI)-
346 anchored cell wall proteins. Our reconstructions of the evolution of these families (Fig. 5c)
347 revealed no expansion but a small contraction (from 17 to 14 copies) in BCZ nodes. Expansions
348 were inferred in the Agaricomycotina and in Saccharomycotina yeasts (*C. albicans*, *P. stipitis*,
349 *D. hansenii*). The expansion in the Agaricomycotina was driven by class1 hydrophobins and
350 homologs of the *C. neoformans* Cfl1 (an adhesive protein with roles in signaling and
351 morphogenesis regulation)⁹⁰. Diversification of these families correlates with the evolution of
352 fruiting bodies and probably reflects the emergence of complex multicellularity⁷. The higher copy
353 numbers in yeast species relate to several yeast-specific adhesin and lectin-like cell wall
354 proteins that contain experimentally characterized adhesive proteins of human pathogenic fungi
355 (e.g. *Candida* spp.)^{91,92}.

356
357 Taken together, the evolution of kinase, receptor and adhesive protein repertoires
358 highlights an important difference between fungi and other multicellular lineages. We observed
359 no significant expansion of such families in filamentous fungi, whereas kinase and adhesion
360 related genes expanded in complex multicellular Agaricomycotina. This might be explained by
361 the two-step nature of the evolution of complex MC in fungi^{7,93} that proceeds through an
362 intermediate complexity level, hyphal MC, as opposed to metazoans, where complex MC
363 evolved in a more direct way¹⁴.



364
 365 Fig. 5. Gene family evolution of Serine-Threonine kinases (a), transmembrane receptors (b) and
 366 adhesion-related genes (c). BCZ nodes (yellow) represent the putative origin of hyphal MC. Bubble size
 367 across the tree is proportional to reconstructed ancestral gene copy number and copy number of extant
 368 species (shown right to the tree). Violin plots for kinases (a) and receptors (b) show copy number
 369 distribution of gene families in multicellular fungi (grey) and metazoans (green).

370 Yeasts retain most genes required for hyphal morphogenesis

371 Yeasts are secondarily simplified organisms with reduced ability to form hyphae and that spend
 372 most of their life cycle as unicells^{16,18,53,94}. Our ancestral character state reconstructions imply
 373 that yeasts derived from filamentous ancestors (Fig. 1a), and thus they represent a classic
 374 example of reduced complexity. They were hypothesized to have lost MC⁹⁵, even though
 375 rudimentary forms of hyphal growth (termed pseudohyphae) exist in most species. We
 376 scrutinized the fate of MC-related genes in five predominantly yeast-like lineages⁹⁴, the
 377 Saccharomycotina, Taphrinomycotina, Pucciniomycotina, Ustilaginomycotina and
 378 Tremellomycotina. Because yeast genomes have undergone extreme streamlining during
 379 evolution, we evaluated gene loss among MC-related genes in comparison to genome-wide
 380 figures of gene loss.

381
 382 Yeast species generally have fewer MC-related genes and reconstructions indicate more
 383 losses than duplications along branches of yeast ancestors (Fig. 6). However, when we
 384 corrected for genome-wide reductions in gene number, we found that hyphal morphogenesis
 385 genes are underrepresented among lost genes compared to other functions (Fig. 6a,
 386 Supplementary Table 7). Most groups of hyphal morphogenesis genes are significantly depleted
 387 ($P < 0.05$, Fisher's exact test) among gene losses in yeast clades (except the
 388 Ustilaginomycotina). We recovered only 6 cases where losses of MC-related genes were
 389 significantly overrepresented ($P < 0.05$, Fisher's exact test, Supplementary Table 7), in proteins

390 related to adhesion and microtubule-based transport. Higher than expected loss rates in such
391 proteins were observed in the Taphrinomycotina, Pucciniomycotina, Tremellomycotina and the
392 Saccharomycotina, suggesting that microtubule-based transport and adhesion-related functions
393 become dispensable for these yeasts clades. Losses in 'microtubule system' are particularly
394 interesting from the perspective of long-range transport of vesicles and nuclei along hyphae.
395 Microtubule system-related genes with reduced repertoires in yeasts include gamma-tubulin
396 complex proteins, kinesins, dynactin, dynein heavy chain (*nudA*), and the dynactin linking
397 protein *ro-2*⁹⁶. Of the five yeast-like clades, the budding and fission yeast lineages show the
398 most gene losses, consistent with the strongest reduction of hyphal growth abilities in these
399 clades. A similar pattern was found for NADPH oxidases, which is consistent with previous
400 reports: concurrent losses in all yeast-like clades, with complete loss of the family in the
401 Saccharomycotina, Ustilaginomycotina, in *S. pombe* and *C. neoformans* (Supplementary Fig.
402 4).

403
404 Altogether 54-65% of MC-related genes were retained in yeast genomes
405 (Supplementary Table 7). For example, hardly any reductions are observed in PI4,5P2 binding
406 proteins (*Slm1*, *Slm2* in *S. cerevisiae*⁹⁷), which are involved in the regulation of actin
407 cytoskeleton organization and endosomal transport, or in class I myosins (*myoA* in *A.*
408 *nidulans*⁹⁸, *myo5* in *S. cerevisiae*⁹⁹) which are localized to the site of polarized growth and
409 involved in secretion and cell wall biogenesis.

410
411 Collectively, these data suggest that hyphal morphogenesis genes in general are
412 dispensable for yeasts to a smaller extent than genes with other functions. This is consistent
413 with most yeast-like fungi being able to switch to hyphal or pseudohyphal growth under certain
414 conditions. The fact that hyphal morphogenesis genes are not statistically significantly enriched
415 among losses compared to genome-wide expectation, however, is not in conflict with a
416 reduction of multicellular abilities in yeast-like fungi. These gene losses do indicate reductions in
417 hyphal growth, although this cutback is smaller compared to other functions in the genome. This
418 in turn suggests, that the ability for multicellular growth is among the functions preferentially
419 retained by yeast-like fungi.

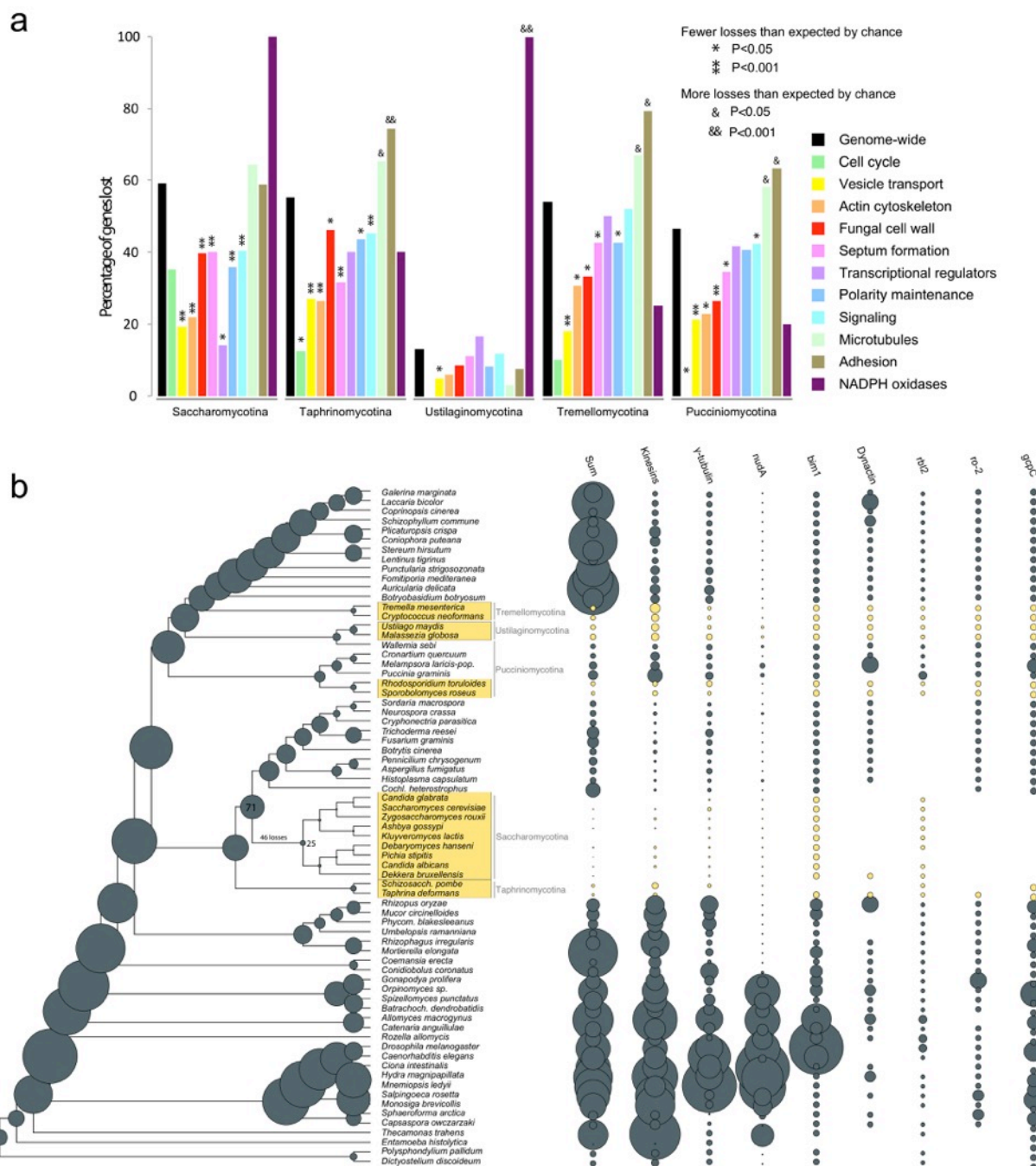


Fig. 6. Secondly simplified yeast-like fungi retain genes for hyphal MC. (a) the percentages of lost genes in main morphogenesis-related categories. Percentages were calculated relative to ancestral copy numbers inferred in the node preceding the origin of 5 yeast-like clades (Saccharomycotina, Taphrinomycotina, Pucciniomycotina, Ustilaginomycotina and Tremellomycotina). Significance of the enrichment of gene losses in each category relative to genome-wide figures of gene loss were determined by Fisher's exact test and is shown above bars. (b) ancestral gene copy number reconstruction of microtubule-based transport genes along the fungal phylogeny. Secondly simplified (yeast-like) clades are highlighted in yellow. Bubble size proportional to reconstructed ancestral and extant gene copy number across 19 gene families. Copy number distribution of each gene family is shown right to the tree.

431 Conclusions

432 We analyzed the genetic underpinnings of the evolution of fungal hyphae. Hyphae are among
433 the most enigmatic fungal structures with a unique multicellular organization, yet their
434 evolutionary origins remained poorly explored. Our ancestral character state reconstructions
435 localized the origin of hyphae to three nodes around the split of Blastocladio-, Chytridio- and
436 Zoopagomycota (BCZ nodes), consistent with previous studies¹⁷ and potential convergence of
437 hypha-like structures in these phyla.

438
439 To understand how the underlying genetics evolved, we identified 362 gene families with
440 known relevance to hyphal morphogenesis (e.g. from knockout studies) and predicted a link to
441 hyphal MC for another 414 families using comparative genomics of 71 species. The
442 evolutionary dynamics of these families shows a mixed picture. A large proportion of families
443 are conserved in all sampled eukaryotes and show very little or no copy number dynamics at all
444 at the origin of multicellular fungi. A second category comprises gene families with a deep
445 eukaryotic origin that show duplications coincident with the evolution of hyphae. However, no
446 families were found that had statistically significantly elevated number of duplications in BCZ
447 nodes, indicating limited evolutionary novelty in these nodes. In the third category there are
448 gene families whose origin mapped to BCZ nodes (RGSs, formins, APSES and Bem1 families).
449 Such gene families could have evolved *de novo* or diverged in sequence so much that similarity
450 is not detectable to homologous non-fungal sequences. We find candidates for both scenarios.
451 For example, the MedA or APSES families contain fungal-specific protein domains; these have
452 conceivably evolved in early fungi and represent fungal-specific innovations. On the other hand,
453 the detected formin and RGS families contained only fungal genes, but their characteristic
454 Interpro domains occur outside of fungi too, possibly reflecting common ancestry, with evidence
455 for homology blurred by sequence divergence.

456
457 We found that several multicellularity-related genes predate the emergence of hyphal
458 MC and were co-opted for hyphal growth during evolution, which mirrors patterns observed in
459 multicellular animals and plants^{6,100,101}. Such observations rise to the hypothesis that in terms of
460 genetic novelty, transitions to multicellularity represent a minor rather than a major evolutionary
461 step¹⁰², an idea that finds support in the observations made here on fungi. Cell polarity
462 maintenance, vesicle trafficking and cytoskeletal systems of unicellular eukaryotes may have
463 turned out to be useful functions in hyphal MC, on which the extreme polarized growth of fungal
464 hyphae could have built during evolution. The phagocytotic machinery was probably exapted for
465 hyphal MC: its original function was most likely lifted by the emergence of a rigid cell wall in
466 early fungi, which probably made the underlying genes dispensable. However, instead of being
467 lost over time, its components got incorporated into hyphal MC.

468
469 Finally, beyond gene family events, certainly other genetic mechanisms (e.g. changes in
470 amino acid sequence and domain composition, changes to biophysical properties of genes) also
471 contributed to the evolution of hyphae. Our analyses of gene architecture revealed significant
472 differences between MC-related genes of unicellular and multicellular fungi, indicating that
473 changes in CDS length or intron content are also relevant for the emergence of hyphal MC¹⁰³.

474 Reports of sequence-level changes and domain shuffling in connection with the evolution of
475 hyphal MC have also been published. There is evidence for fungal kinesins being 2x more
476 processive than other eukaryotic kinesins¹⁰⁴ - probably in response to needs of long range
477 transport along the hyphal axis. Similarly, class V and VII chitin synthases gained a myosin
478 motor domain in early fungi, providing higher efficiency in polarized chitin synthesis¹⁰⁵⁻¹⁰⁷.

479
480 Taken together, our results suggest that multiple mechanisms probably contributed to
481 the evolution of hyphal MC, including changes in gene structure, gene duplications, *de novo*
482 gene family birth, and co-option/neofunctionalization. Compared to other multicellular lineages,
483 the evolution of fungi shows several unique patterns. While the expansion of adhesion and
484 signal transduction mechanisms is shared by most colonial and aggregative multicellular
485 lineages examined so far^{3,9,19,108-110}, we did not find evidence for this in fungi. This could be
486 explained by the peculiar life history of fungal hyphae, which shares similarity with only
487 Oomycota. While adhesion might not be key in vegetative hyphae, there is plenty of evidence
488 for active communication between neighboring hyphae¹¹¹⁻¹¹³. It is possible that the main modes
489 of communication in fungal hyphae are not linked to cell surface receptors, might be related to
490 volatiles (such as farnesol^{80,114,115}) or are not known yet. These observations suggest that
491 multicellularity in fungi differs considerably from that in other lineages and raises the possibility
492 that hyphal MC should be considered a third, qualitatively different way in addition to the
493 aggregative and clonal modes of evolving MC. Subjective categorizations aside, hyphal MC
494 represents a highly successful adaptation to terrestrial life and comparative genomics opens the
495 door for discussions on whether major phenotypic transitions represent - in terms of genetic
496 novelty - a major or a minor transition.

497

498 Methods

499 Organismal phylogeny

500 We assembled a dataset containing whole proteomes of 71 species and performed all-vs-all
501 blast using mpiBLAST 1.6.0¹¹⁶. We omitted Microsporidia from the dataset due to the high rate
502 of evolution of this group. Proteins were clustered into gene families with Markov Cluster
503 Algorithm (MCL)¹¹⁷ with an inflation parameter of 2.0. Clusters with at least 50% taxon
504 occupancy were chosen and were aligned by PRANK 140603¹¹⁸ while trimAl 1.4.rev15¹¹⁹ was
505 used to remove poorly aligned regions from the multiple sequence alignments using the
506 parameter -gt 0.2. Approximately-maximum-likelihood gene trees were inferred by FastTree¹²⁰
507 using the LG+CAT model (-lg -cat20), and the option -gamma to compute a Gamma20-based
508 likelihoods. Using a custom-made Perl script we excluded gene trees with deep paralogs to
509 identify single-copy genes. Alignments of single-copy gene clusters were concatenated into a
510 supermatrix and a species tree was estimated using RAxML 8.2.4¹²¹ under the
511 PROTGAMMAWAG model. The model was partitioned by gene. Bootstrapping was performed
512 on the dataset in 100 replicates.

513

514 Ancestral character state reconstructions

515 The 71 species were coded for their ability to form hyphae, either as hyphal or non-hyphal.
516 Species that could not be unambiguously assigned to hyphal or non-hyphal (*Catenaria*
517 *anguillulae*) and those with the ability to grow either as hyphae or unicells (most yeasts) were
518 coded as uncertain. Bayesian MCMC reconstruction of ancestral character states was
519 performed under the threshold model¹²² using Bayesian MCMC with the “ancThresh” function in
520 phytools v0.6-60¹²³ in R¹²⁴. The number of generations for MCMC was set to 1,000,000, and the
521 method “mcmc” was used with the Brownian motion as the model for the evolution of the
522 liability. Burn-in parameter was set to default. Convergence was checked by inspecting
523 likelihood values through time.

524

525 **Analyses of Gene family evolution**

526 To investigate the evolutionary dynamics of gene families containing hyphal morphogenesis-
527 related genes, we performed all-vs-all blast (NCBI Blast 2.7.1+) ¹²⁵ for proteomes of the 71
528 species and did sequence similarity-based protein clustering by following the MCL clustering
529 protocol¹¹⁷ used by Ohm et al 2012¹²⁶. The resulting protein clusters were aligned by PRANK
530 140603¹¹⁸ with default parameters, and ambiguously aligned regions were removed using trimAl
531 1.4.rev15¹¹⁹ with the argument -gt 0.2. MAFFT v7.222¹²⁷ (option --auto) was used as an
532 alternative alignment tool for clusters that could not be aligned by PRANK due to computational
533 limitations (80 out of 34032 clusters). Maximum Likelihood inference of gene trees and
534 calculation of Shimodaira-Hasegawa-like branch support values were carried out in RAxML
535 8.2.4¹²⁸ under the PROTGAMMAWAG model of protein evolution. The calculated SH-like
536 branch support values were used in gene tree-species tree reconciliation in Notung-2.9¹²⁹. An
537 edge-weight threshold of 0.9 was used, as SH-like support values are usually less conservative
538 than ML bootstrap values (where 70% is usually taken as indication of strong support).
539 Reconciliation was performed on the maximum likelihood gene trees and the ML species tree
540 for the 71 species as input. We reconstructed the gene duplication/loss dynamics of gene
541 families along the species tree using respective scripts from the COMPARE pipeline^{94,130}. The
542 numbers of gains and losses for each gene family and for each branch of the species tree were
543 recorded and mapped on the species tree. Ancestral gene copy numbers were calculated for
544 every internal node, summing the mapped duplications and losses across the species tree.
545 Mappings were generated for each of the functional groups and also for kinases, adhesion-
546 related proteins, receptors as well as for all gene families across the 71 genomes.

547

548 To test if genes related to hyphal MC experience an episode of increased duplication
549 rate in nodes where hyphal growth putatively originated (BCZ nodes), we performed gene
550 duplication enrichment analysis for each of the 362 families and for functional groups. To test if
551 a cluster or a functional group shows significantly more or less duplications than expected by
552 chance in BCZ nodes, we run two-tailed Fisher’s exact tests ($p < 0.05$). We compared the
553 number of duplications mapped to BCZ nodes for a given gene family to the genome-wide
554 number of duplications in BCZ nodes, using total number of duplications across the tree as a
555 reference.

556

557 **Analyses of key multicellularity-related genes**

558 The above strategy was used to reconstruct the evolution of kinase, receptor and adhesion-
559 related gene families. Protein clusters containing kinase genes, both serine-threonine kinases
560 and histidine kinases, were collected based on InterPro domains. Identification of serine-
561 threonine kinases and histidine kinases followed Park et al 2011¹³¹ and Herivaux et al 2016⁸⁸,
562 respectively. Classification of histidine kinases followed Defosse et al⁸⁷.

563
564 Families of adhesive proteins were identified based on experimentally characterized
565 genes collected from the literature. We identified 45 genes, which mostly grouped into
566 flocculins, lectins, hydrophobins and other (GPI)-modified cell wall adhesins. We identified
567 receptor genes based on InterPro domains that are annotated with the gene ontology term
568 'receptor activity' (but not 'receptor binding' or other terms indicative of indirect relationships to
569 receptor function), resulting in 27 IPR terms (IPR000161, IPR000276, IPR000337, IPR000363,
570 IPR000366, IPR000481, IPR000832, IPR000848, IPR001103, IPR001105, IPR001499,
571 IPR001546, IPR001946, IPR002011, IPR002185, IPR002280, IPR002455, IPR002456,
572 IPR003110, IPR003292, IPR003980, IPR003982, IPR005386, IPR006211, IPR017978,
573 IPR017979, IPR017981).

574 575 **Analyses of phagocytosis-related genes**

576 We collected information on phagocytosis-related genes from recent reviews on
577 *Dictyostelium*^{65,66}, identified the corresponding genes of this species in our dataset and the
578 protein clusters that contained homologs of the identified genes. Mapping of gene duplications
579 and losses along the species tree was done as described above.

580 581 **Genome-wide screen for putative hyphal multicellularity-related gene families**

582 To identify gene families with increased rates of gene duplication coinciding with the origin of
583 hyphal MC, we set up a pipeline that tests for higher than expected rate of duplication in nodes
584 of the species tree to which the origin of hyphae could be located (BCZ nodes). For each gene
585 family, gene duplication rates in BCZ nodes were compared to duplication rates of the same
586 family in other parts of the species tree (nodes before and after BCZ nodes). Gene duplication
587 rates were computed by dividing the number of reconstructed duplications for a given branch by
588 the length of that branch using a custom Perl script. Terminal duplications and duplications
589 mapped to metazoan ancestors were excluded from the analysis. The resulting
590 node×duplication rate matrix was analyzed by a two-factor permutation ANOVA¹³² with degrees
591 of freedom DFT=2, in R, with $P < 0.05$ considered as significant. We further required that the
592 detected clusters be conserved (≥ 1 copy) in at least 70% of filamentous fungi.

593 594 **Analyses of gene losses in yeast-like fungi**

595 We analyzed gene losses in five yeast-like lineages by comparing the number of losses
596 genome-wide, to the numbers of losses in hyphal morphogenesis related genes (actin
597 cytoskeleton regulation, polarity maintenance, cell wall biogenesis/remodelling, septation and
598 septal plugging, signal transduction, transcriptional regulation, vesicle transport, microtubule-
599 based transport and cell cycle regulation) relative to ancestral copy numbers. P-values were
600 calculated by Fisher's exact test, with $P < 0.05$ considered as significant. The percentage of
601 genes retained in yeast genomes was calculated for every functional category by comparing

602 ancient gene-copy number prior to the emergence of yeast-like lineages to the average gene
603 copy-number of terminals.

604

605 **Statistical analysis of genomic features**

606 An R script (available upon request) was written to generate coding sequence (CDS)/intron
607 statistics (strand, order, length, count) based on genome annotations of the 71 species. CDS
608 feature coordinates for each gene were extracted and subsequently used to calculate intron
609 coordinates. Statistical significance of the differences between the gene, CDS and intron
610 lengths of 4 unicellular and 39 multicellular fungi was investigated by independent two-tailed
611 Welch's t-test with pooled variance estimation (`var.equal=FALSE`), using the `t.test` function in R.

612 **Data availability**

613 Files associated with this paper (including gene and species trees, gene duplication/loss
614 catalogs) have been deposited in Dryad (Accession number, *to be provided upon publication*).

615 **Acknowledgements**

616 The authors are thankful to Sándor Kocsubé for his help in crafting figures. This work was
617 supported by the 'Momentum' program of the Hungarian Academy of Sciences (contract No.
618 LP2014/12 to L.G.N.) and the European Research Council (grant no. 758161 to L.G.N.). E.K.
619 acknowledges support from the National Talent Program of the Ministry of Human Capacities
620 (contract No. NTP-NFTÖ-16-0566) and the Young Researchers Program of the Hungarian
621 Academy of Sciences. N.T. acknowledges support from Japan Society for the Promotion of
622 Science (JSPS) KAKENHI (grant number: 18K05545) and Japan Science and Technology
623 Agency (JST) ERATO (grant number: JPMJER1502).

624 **Author contributions**

625 E.K. and N.G.L. conceived the study. E.K. collected literature data on morphogenesis-related
626 genes. E.K. and A.N.P. inferred species trees, B.B. performed clustering, E.K., K.K., T.K., Z.M.
627 and T.V. analyzed gene family evolution. B.H. analyzed gene structural changes. E.K., M.R.,
628 N.T. and N.G.L. interpreted the results and wrote the paper. All authors have read and
629 commented on the manuscript.

630 **Competing interests**

631 The authors declare no competing interests.

632 **References**

- 633 1. Szathmáry, E. Toward major evolutionary transitions theory 2.0. *Proc. Natl. Acad. Sci. U.*
634 *S. A.* **112**, 10104–11 (2015).
- 635 2. Rokas, A. The Origins of Multicellularity and the Early History of the Genetic Toolkit For

- 636 Animal Development. *Annu. Rev. Genet.* **42**, 235–251 (2008).
- 637 3. Abedin, M. & King, N. Diverse evolutionary paths to cell adhesion. *Trends Cell Biol.* **20**,
638 734–42 (2010).
- 639 4. Coates, J. C., Aiman, U.-E. & Charrier, B. Understanding “green” multicellularity:
640 do seaweeds hold the key? *Front. Plant Sci.* **5**, 737 (2015).
- 641 5. Brunet, T. & King, N. The Origin of Animal Multicellularity and Cell Differentiation. *Dev*
642 *Cell* **43**, 124–140 (2017).
- 643 6. Sebé-Pedrós, A., Degnan, B. M. & Ruiz-Trillo, I. The origin of Metazoa: a unicellular
644 perspective. *Nat. Rev. Genet.* **18**, 498–512 (2017).
- 645 7. Nagy, L. G., Kovács, G. M. & Krizsán, K. Complex multicellularity in fungi: evolutionary
646 convergence, single origin, or both? *Biol. Rev.* (2018). doi:10.1111/brv.12418
- 647 8. Brown, M. W., Spiegel, F. W. & Silberman, J. D. Phylogeny of the “Forgotten”
648 Cellular Slime Mold, *Fonticula alba*, Reveals a Key Evolutionary Branch within
649 Opisthokonta. *Mol. Biol. Evol.* **26**, 2699–2709 (2009).
- 650 9. Sebé-Pedrós, A. *et al.* Regulated aggregative multicellularity in a close unicellular relative
651 of metazoa. *Elife* **2**, e01287 (2013).
- 652 10. Glöckner, G. *et al.* The multicellularity genes of dictyostelid social amoebas. *Nat.*
653 *Commun.* **7**, 12085 (2016).
- 654 11. Ruiz-Trillo, I. *et al.* The origins of multicellularity: a multi-taxon genome initiative. *Trends*
655 *Genet.* **23**, 113–118 (2007).
- 656 12. Fairclough, S. R. *et al.* Premetazoan genome evolution and the regulation of cell
657 differentiation in the choanoflagellate *Salpingoeca rosetta*. *Genome Biol.* **14**, R15 (2013).
- 658 13. Blackwell, M. The Fungi: 1, 2, 3 ... 5.1 million species? *Am. J. Bot.* **98**, 426–438 (2011).
- 659 14. Niklas, K. J. & Newman, S. A. The origins of multicellular organisms. *Evol. Dev.* **15**, 41–
660 52 (2013).
- 661 15. Harris, S. D. Branching of fungal hyphae: regulation, mechanisms and comparison with
662 other branching systems. *Mycologia* **100**, 823–832 (2008).
- 663 16. Stajich, J. E. *et al.* The Fungi. *Curr. Biol.* **19**, R840–R845 (2009).
- 664 17. Dee, J. M., Mollicone, M., Longcore, J. E., Roberson, R. W. & Berbee, M. L. Cytology and
665 molecular phylogenetics of Monoblepharidomycetes provide evidence for multiple
666 independent origins of the hyphal habit in the Fungi. *Mycologia* **107**, 710–728 (2015).
- 667 18. Nagy, L. G. *et al.* Six Key Traits of Fungi: Their Evolutionary Origins and Genetic Bases.
668 in *The Fungal Kingdom* **5**, 35–56 (American Society of Microbiology, 2017).
- 669 19. Sebé-Pedrós, A., Degnan, B. M. & Ruiz-Trillo, I. The origin of Metazoa: A unicellular
670 perspective. *Nature Reviews Genetics* **18**, 498–512 (2017).
- 671 20. Svedberg, J. *et al.* Convergent evolution of complex genomic rearrangements in two
672 fungal meiotic drive elements. *Nat. Commun.* **9**, 4242 (2018).
- 673 21. Fricker, M. D., Heaton, L. L. M., Jones, N. S. & Boddy, L. The Mycelium as a Network.
674 *Microbiol. Spectr.* **5**, (2017).
- 675 22. Richards, T. A., Leonard, G. & Wideman, J. G. What Defines the “Kingdom”
676 Fungi? *Microbiol. Spectr.* **5**, (2017).
- 677 23. Sekimoto, S., Rochon, D., Long, J. E., Dee, J. M. & Berbee, M. L. A multigene phylogeny
678 of *Olpidium* and its implications for early fungal evolution. *BMC Evol. Biol.* **11**, 331 (2011).
- 679 24. Ryan, O. *et al.* Global gene deletion analysis exploring yeast filamentous growth. *Science*
680 **337**, 1353–6 (2012).
- 681 25. Stajich, J. E. *et al.* Insights into evolution of multicellular fungi from the assembled
682 chromosomes of the mushroom *Coprinopsis cinerea* (*Coprinus cinereus*). *Proc. Natl.*
683 *Acad. Sci. U. S. A.* **107**, 11889–94 (2010).
- 684 26. Kűes, U., Khonsuntia, W. & Subba, S. Complex fungi. *Fungal Biol. Rev.* **32**, 205–218
685 (2018).
- 686 27. Pöggeler, S., Nowrousian, M., Teichert, I., Beier, A. & Kűck, U. Fruiting-Body

- 687 Development in Ascomycetes. in *Physiology and Genetics* 1–56 (Springer International
688 Publishing, 2018). doi:10.1007/978-3-319-71740-1_1
- 689 28. Knoll, A. H. The Multiple Origins of Complex Multicellularity. *Earth Planet. Sci.* **39**, 217–
690 239 (2011).
- 691 29. Verstrepen, K. J., Reynolds, T. B. & Fink, G. R. Origins of variation in the fungal cell
692 surface. *Nat. Rev. Microbiol.* **2**, 533–540 (2004).
- 693 30. King, N., Hittinger, C. T. & Carroll, S. B. Evolution of Key Cell Signaling and Adhesion
694 Protein Families Predates Animal Origins. *Science* (80-.). **301**, 361–363 (2003).
- 695 31. Miller, W. T. Tyrosine kinase signaling and the emergence of multicellularity. *Biochim.*
696 *Biophys. Acta - Mol. Cell Res.* **1823**, 1053–1057 (2012).
- 697 32. Mendoza, A. de *et al.* Transcription factor evolution in eukaryotes and the assembly of
698 the regulatory toolkit in multicellular lineages. *Proc. Natl. Acad. Sci.* **110**, E4858–E4866
699 (2013).
- 700 33. Harris, S. D. *et al.* Polarisome meets Spitzenkörper: microscopy, genetics, and genomics
701 converge. *Eukaryot. Cell* **4**, 225–9 (2005).
- 702 34. Steinberg, G. Hyphal growth: a tale of motors, lipids, and the Spitzenkörper. *Eukaryot.*
703 *Cell* **6**, 351–60 (2007).
- 704 35. Sudbery, P. E. Regulation of polarised growth in fungi. *Fungal Biol. Rev.* **22**, 44–55
705 (2008).
- 706 36. Harris, S. D. *et al.* Morphology and development in *Aspergillus nidulans*: A complex
707 puzzle. *Fungal Genet. Biol.* **46**, S82–S92 (2009).
- 708 37. Steinberg, G., Peñalva, M. A., Riquelme, M., Wosten, H. & Harris, S. D. Cell Biology of
709 Hyphal Growth. *Microbiol. Spectr.* **5**, 1–34 (2017).
- 710 38. Riquelme, M. *et al.* Fungal Morphogenesis, from the Polarized Growth of Hyphae to
711 Complex Reproduction and Infection Structures. *Microbiol. Mol. Biol. Rev.* **82**, e00068-17
712 (2018).
- 713 39. Fischer, R., Zekert, N. & Takeshita, N. Polarized growth in fungi – interplay between the
714 cytoskeleton, positional markers and membrane domains. *Mol. Microbiol.* **68**, 813–826
715 (2008).
- 716 40. Schultzhause, Z. S. & Shaw, B. D. Endocytosis and exocytosis in hyphal growth. *Fungal*
717 *Biol. Rev.* **29**, 43–53 (2015).
- 718 41. Schuster, M. *et al.* Co-delivery of cell-wall-forming enzymes in the same vesicle for
719 coordinated fungal cell wall formation. *Nat. Microbiol.* **1**, 16149 (2016).
- 720 42. Momany, M. Polarity in filamentous fungi: establishment, maintenance and new axes.
721 *Curr. Opin. Microbiol.* **5**, 580–585 (2002).
- 722 43. Virag, A. & Harris, S. D. The Spitzenkörper: a molecular perspective. *Mycol. Res.* **110**, 4–
723 13 (2006).
- 724 44. Wendland, J. Comparison of Morphogenetic Networks of Filamentous Fungi and Yeast.
725 *Fungal Genet. Biol.* **34**, 63–82 (2001).
- 726 45. Palecek, S. P., Kron, S. J. & Parikh, A. S. Sensing, signalling and integrating physical
727 processes during *Saccharomyces cerevisiae* invasive and filamentous growth.
728 *Microbiology* **148**, 893–907 (2002).
- 729 46. Bahn, Y.-S. *et al.* Sensing the environment: lessons from fungi. *Nat. Rev. Microbiol.* **5**,
730 57–69 (2007).
- 731 47. Biswas, S., Van Dijck, P. & Datta, A. Environmental sensing and signal transduction
732 pathways regulating morphopathogenic determinants of *Candida albicans*. *Microbiol. Mol.*
733 *Biol. Rev.* **71**, 348–76 (2007).
- 734 48. Román, E., Arana, D. M., Nombela, C., Alonso-Monge, R. & Pla, J. MAP kinase
735 pathways as regulators of fungal virulence. *Trends Microbiol.* **15**, 181–190 (2007).
- 736 49. Sudbery, P. E. Growth of *Candida albicans* hyphae. *Nat. Rev. Microbiol.* **9**, 737–748
737 (2011).

- 738 50. Berbee, M. L., James, T. Y. & Strullu-Derrien, C. Early Diverging Fungi: Diversity and
739 Impact at the Dawn of Terrestrial Life. *Annu. Rev. Microbiol.* **71**, 41–60 (2017).
- 740 51. Strullu-Derrien, C. *et al.* New insights into the evolutionary history of Fungi from a 407 Ma
741 Blastocladiomycota fossil showing a complex hyphal thallus. *Philos. Trans. R. Soc. B*
742 *Biol. Sci.* **373**, 20160502 (2018).
- 743 52. Redecker, D., Kodner, R. & Graham, L. E. Glomalean fungi from the Ordovician. *Science*
744 **289**, 1920–1 (2000).
- 745 53. Harris, S. D. Hyphal morphogenesis: an evolutionary perspective. *Fungal Biol.* **115**, 475–
746 484 (2011).
- 747 54. Powell, M. J. Blastocladiomycota. in *Handbook of the Protists* 1497–1521 (Springer
748 International Publishing, 2017). doi:10.1007/978-3-319-28149-0_17
- 749 55. Chang, Y. *et al.* Phylogenomic Analyses Indicate that Early Fungi Evolved Digesting Cell
750 Walls of Algal Ancestors of Land Plants. *Genome Biol. Evol.* **7**, 1590–1601 (2015).
- 751 56. Spatafora, J. W. *et al.* The Fungal Tree of Life: From Molecular Systematics to Genome-
752 Scale Phylogenies. in *The Fungal Kingdom* **5**, 3–34 (American Society of Microbiology,
753 2017).
- 754 57. Ahrendt, S. R. *et al.* Leveraging single-cell genomics to expand the fungal tree of life. *Nat.*
755 *Microbiol.* **3**, 1417–1428 (2018).
- 756 58. Spatafora, J. W. *et al.* A phylum-level phylogenetic classification of zygomycete fungi
757 based on genome-scale data. *Mycologia* **108**, 1028–1046 (2016).
- 758 59. Gravelat, F. N. *et al.* *Aspergillus fumigatus* MedA governs adherence, host cell
759 interactions and virulence. *Cell. Microbiol.* **12**, 473–488 (2010).
- 760 60. Zhao, Y. *et al.* The APSES family proteins in fungi: Characterizations, evolution and
761 functions. *Fungal Genet. Biol.* **81**, 271–280 (2015).
- 762 61. Lichius, A., Yáñez-Gutiérrez, M. E., Read, N. D. & Castro-Longoria, E. Comparative Live-
763 Cell Imaging Analyses of SPA-2, BUD-6 and BNI-1 in *Neurospora crassa* Reveal Novel
764 Features of the Filamentous Fungal Polarisome. *PLoS One* **7**, e30372 (2012).
- 765 62. Bender, A. & Pringle, J. R. Use of a screen for synthetic lethal and multicopy suppressor
766 mutants to identify two new genes involved in morphogenesis in *Saccharomyces*
767 *cerevisiae*. *Mol. Cell. Biol.* **11**, 1295–305 (1991).
- 768 63. Madden, K. & Snyder, M. CELL POLARITY AND MORPHOGENESIS IN BUDDING
769 YEAST. *Annu. Rev. Microbiol.* **52**, 687–744 (1998).
- 770 64. Fujita, A. *et al.* Rax1, a protein required for the establishment of the bipolar budding
771 pattern in yeast. *Gene* **327**, 161–169 (2004).
- 772 65. Bozzaro, S., Bucci, C. & Steinert, M. Chapter 6 Phagocytosis and Host–Pathogen
773 Interactions in *Dictyostelium* with a Look at Macrophages. in *International review of cell*
774 *and molecular biology* **271**, 253–300 (2008).
- 775 66. Rivero, F. Endocytosis and the Actin Cytoskeleton in *Dictyostelium discoideum*. *Int. Rev.*
776 *Cell Mol. Biol.* **267**, 343–397 (2008).
- 777 67. Mao, Y. & Finnemann, S. C. Regulation of phagocytosis by Rho GTPases. *Small*
778 *GTPases* **6**, 89 (2015).
- 779 68. May, R. C., Caron, E., Hall, A. & Machesky, L. M. Involvement of the Arp2/3 complex in
780 phagocytosis mediated by FcγR or CR3. *Nat. Cell Biol.* **2**, 246–248 (2000).
- 781 69. Epp, E. *et al.* Forward genetics in *Candida albicans* that reveals the Arp2/3 complex is
782 required for hyphal formation, but not endocytosis. *Mol. Microbiol.* **75**, 1182–1198 (2010).
- 783 70. Hope, H., Bogliolo, S., Arkowitz, R. A. & Bassilana, M. Activation of Rac1 by the Guanine
784 Nucleotide Exchange Factor Dck1 Is Required for Invasive Filamentous Growth in the
785 Pathogen *Candida albicans*. *Mol. Biol. Cell* **19**, 3638–3651 (2008).
- 786 71. Torruella, G. *et al.* Global transcriptome analysis of the aphelid *Paraphelidium tribonemae*
787 supports the phagotrophic origin of fungi. *Commun. Biol.* **1**, 231 (2018).
- 788 72. Kollmar, M., Lbik, D. & Enge, S. Evolution of the eukaryotic ARP2/3 activators of the

- 789 WASP family: WASP, WAVE, WASH, and WHAMM, and the proposed new family
790 members WAWH and WAML. *BMC Res. Notes* **5**, 88 (2012).
- 791 73. Chen, T. *et al.* Multigenerational Cortical Inheritance of the Rax2 Protein in Orienting
792 Polarity and Division in Yeast. *Science (80-.)*. **290**, 1975–1978 (2000).
- 793 74. Gonía, S. *et al.* Rax2 is important for directional establishment of growth sites, but not for
794 reorientation of growth axes, during *Candida albicans* hyphal morphogenesis. *Fungal*
795 *Genet. Biol.* **56**, 116–24 (2013).
- 796 75. Choi, E., Lee, K. & Song, K. Function of rax2p in the polarized growth of fission yeast.
797 *Mol. Cells* **22**, 146–53 (2006).
- 798 76. Borkovich, K. A. *et al.* Lessons from the genome sequence of *Neurospora crassa*: tracing
799 the path from genomic blueprint to multicellular organism. *Microbiol. Mol. Biol. Rev.* **68**,
800 1–108 (2004).
- 801 77. Corrochano, L. M. *et al.* Expansion of Signal Transduction Pathways in Fungi by
802 Extensive Genome Duplication. *Curr. Biol.* **26**, 1577–1584 (2016).
- 803 78. Basu, R. & Chang, F. Characterization of Dip1p Reveals a Switch in Arp2/3-Dependent
804 Actin Assembly for Fission Yeast Endocytosis. *Curr. Biol.* **21**, 905–916 (2011).
- 805 79. Wagner, A. R., Luan, Q., Liu, S.-L. & Nolen, B. J. Dip1 defines a class of Arp2/3 complex
806 activators that function without preformed actin filaments. *Curr. Biol.* **23**, 1990–8 (2013).
- 807 80. Nickerson, K. W., Atkin, A. L. & Hornby, J. M. Quorum Sensing in Dimorphic Fungi:
808 Farnesol and Beyond. *Appl. Environ. Microbiol.* **72**, 3805–3813 (2006).
- 809 81. Beaulieu, J. M. & O’Meara, B. C. Detecting Hidden Diversification Shifts in Models of
810 Trait-Dependent Speciation and Extinction. *Syst. Biol.* **65**, 583–601 (2016).
- 811 82. Richards, T. A. & Talbot, N. J. Osmotrophy. *Curr. Biol.* **28**, R1179–R1180 (2018).
- 812 83. Lim, W. A. & Pawson, T. Phosphotyrosine Signaling: Evolving a New Cellular
813 Communication System. *Cell* **142**, 661–667 (2010).
- 814 84. Suga, H. *et al.* Genomic survey of premetazoans shows deep conservation of
815 cytoplasmic tyrosine kinases and multiple radiations of receptor tyrosine kinases. *Sci.*
816 *Signal.* **5**, (2012).
- 817 85. de Mendoza, A., Sebé-Pedrós, A. & Ruiz-Trillo, I. The Evolution of the GPCR Signaling
818 System in Eukaryotes: Modularity, Conservation, and the Transition to Metazoan
819 Multicellularity. *Genome Biol. Evol.* **6**, 606–619 (2014).
- 820 86. Krizsan, K. *et al.* Transcriptomic atlas of mushroom development highlights an
821 independent origin of complex multicellularity. *bioRxiv* 349894 (2018).
822 doi:10.1101/349894
- 823 87. Defosse, T. A. *et al.* Hybrid histidine kinases in pathogenic fungi. *Mol. Microbiol.* **95**, 914–
824 924 (2015).
- 825 88. Hérivaux, A. *et al.* Major Sensing Proteins in Pathogenic Fungi: The Hybrid Histidine
826 Kinase Family. *PLoS Pathog.* **12**, e1005683 (2016).
- 827 89. Kirk, D. L. A twelve-step program for evolving multicellularity and a division of labor.
828 *BioEssays* **27**, 299–310 (2005).
- 829 90. Wang, L., Zhai, B. & Lin, X. The Link between Morphotype Transition and Virulence in
830 *Cryptococcus neoformans*. *PLoS Pathog.* **8**, e1002765 (2012).
- 831 91. Kempf, M. *et al.* Disruption of the GPI Protein-Encoding Gene IFF4 of *Candida albicans*
832 Results in Decreased Adherence and Virulence. *Mycopathologia* **168**, 73–77 (2009).
- 833 92. Moreno-Ruiz, E. *et al.* The GPI-modified proteins Pga59 and Pga62 of *Candida albicans*
834 are required for cell wall integrity. *Microbiology* **155**, 2004–2020 (2009).
- 835 93. Nagy, L. G. Evolution: Complex Multicellular Life with 5,500 Genes. *Curr. Biol.* **27**, R609–
836 R612
- 837 94. Nagy, L. G. *et al.* Latent homology and convergent regulatory evolution underlies the
838 repeated emergence of yeasts. *Nat. Commun.* **5**, 4471 (2014).
- 839 95. Shen, X.-X. *et al.* Tempo and Mode of Genome Evolution in the Budding Yeast

- 840 Subphylum. *Cell* **175**, 1533–1545.e20 (2018).
- 841 96. Vierula, P. J. & Mais, J. M. A gene required for nuclear migration in *Neurospora crassa*
842 codes for a protein with cysteine-rich, LIM/RING-like domains. *Mol. Microbiol.* **24**, 331–40
843 (1997).
- 844 97. Fadri, M., Daquinag, A., Wang, S., Xue, T. & Kunz, J. The Pleckstrin Homology Domain
845 Proteins Slm1 and Slm2 Are Required for Actin Cytoskeleton Organization in Yeast and
846 Bind Phosphatidylinositol-4,5-Bisphosphate and TORC2. *Mol. Biol. Cell* **16**, 1883–1900
847 (2005).
- 848 98. McGoldrick, C. A., Gruver, C. & May, G. S. myoA of *Aspergillus nidulans* encodes an
849 essential myosin I required for secretion and polarized growth. *J. Cell Biol.* **128**, 577–87
850 (1995).
- 851 99. Goodson, H. V., Anderson, B. L., Warrick, H. M., Pon, L. A. & Spudich, J. A. Synthetic
852 lethality screen identifies a novel yeast myosin I gene (MYO5): myosin I proteins are
853 required for polarization of the actin cytoskeleton. *J. Cell Biol.* **133**, 1277–91 (1996).
- 854 100. Prochnik, S. E. *et al.* Genomic analysis of organismal complexity in the multicellular green
855 alga *volvox carteri*. *Science (80-)*. **329**, 223–226 (2010).
- 856 101. Richter, D. J., Fozouni, P., Eisen, M. B. & King, N. Gene family innovation, conservation
857 and loss on the animal stem lineage. *Elife* **7**, (2018).
- 858 102. Grosberg, R. K. & Strathmann, R. R. The Evolution of Multicellularity: A Minor Major
859 Transition? *Annu. Rev. Ecol. Evol. Syst.* **38**, 621–654 (2007).
- 860 103. Lozada-Chávez, I., Stadler, P. F. & Prohaska, S. J. Genome-wide features of introns are
861 evolutionary decoupled among themselves and from genome size throughout Eukarya.
862 *bioRxiv* 283549 (2018). doi:10.1101/283549
- 863 104. Lakämper, S., Kallipolitou, A., Woehlike, G., Schliwa, M. & Meyhöfer, E. Single fungal
864 kinesin motor molecules move processively along microtubules. *Biophys. J.* **84**, 1833–43
865 (2003).
- 866 105. Fujiwara, M., Horiuchi, H., Ohta, A. & Takagi, M. A Novel Fungal Gene Encoding Chitin
867 Synthase with a Myosin Motor-like Domain. *Biochem. Biophys. Res. Commun.* **236**, 75–
868 78 (1997).
- 869 106. Takeshita, N., Yamashita, S., Ohta, A. & Horiuchi, H. *Aspergillus nidulans* class V and VI
870 chitin synthases CsmA and CsmB, each with a myosin motor-like domain, perform
871 compensatory functions that are essential for hyphal tip growth. *Mol. Microbiol.* **59**, 1380–
872 1394 (2006).
- 873 107. Sebé-Pedrós, A., Grau-Bové, X., Richards, T. A. & Ruiz-Trillo, I. Evolution and
874 Classification of Myosins, a Paneukaryotic Whole-Genome Approach. *Genome Biol. Evol.*
875 **6**, 290–305 (2014).
- 876 108. Abedin, M. & King, N. The premetazoan ancestry of cadherins. *Science (80-)*. **319**, 946–
877 948 (2008).
- 878 109. Niklas, K. J. & Newman, S. A. The origins of multicellular organisms. *Evol Dev* **15**, 41–52
879 (2013).
- 880 110. Grau-Bové, X. *et al.* Dynamics of genomic innovation in the unicellular ancestry of
881 animals. *Elife* **6**, (2017).
- 882 111. Dettmann, A., Heilig, Y., Valerius, O., Ludwig, S. & Seiler, S. Fungal Communication
883 Requires the MAK-2 Pathway Elements STE-20 and RAS-2, the NRC-1 Adapter STE-50
884 and the MAP Kinase Scaffold HAM-5. *PLoS Genet.* **10**, e1004762 (2014).
- 885 112. Fischer, M. S., Wu, V. W., Lee, J. E., O'Malley, R. C. & Glass, N. L. Regulation of Cell-to-
886 Cell Communication and Cell Wall Integrity by a Network of MAP Kinase Pathways and
887 Transcription Factors in *Neurospora crassa*. *Genetics* **209**, 489–506 (2018).
- 888 113. Serrano, A. *et al.* Spatio-temporal MAPK dynamics mediate cell behavior coordination
889 during fungal somatic cell fusion. *J. Cell Sci.* **131**, jcs.213462 (2018).
- 890 114. Albuquerque, P. & Casadevall, A. Quorum sensing in fungi—a review. *Med. Mycol.* **50**,

- 891 337–45 (2012).
892 115. Cottier, F. & Mühlischlegel, F. A. Communication in Fungi. *Int. J. Microbiol.* **2012**, 9
893 (2012).
894 116. Darling, A. E., Carey, L. & Feng, W. The Design , Implementation , and Evaluation of
895 mpiBLAST. *Proc. Clust.* **2003**, 13–15 (2003).
896 117. van Dongen, S. Graph clustering by flow simulation. *Graph Stimul. by flow Clust.* **PhD**
897 **thesis**, University of Utrecht (2000).
898 118. Löytynoja, A. Phylogeny-aware alignment with PRANK. in 155–170 (Humana Press,
899 Totowa, NJ, 2014). doi:10.1007/978-1-62703-646-7_10
900 119. Capella-Gutierrez, S., Silla-Martinez, J. M. & Gabaldon, T. trimAl: a tool for automated
901 alignment trimming in large-scale phylogenetic analyses. *Bioinformatics* **25**, 1972–1973
902 (2009).
903 120. Price, M. N., Dehal, P. S. & Arkin, A. P. FastTree: Computing Large Minimum Evolution
904 Trees with Profiles instead of a Distance Matrix. *Mol. Biol. Evol.* **26**, 1641–1650 (2009).
905 121. Stamatakis, A. RAxML-VI-HPC: maximum likelihood-based phylogenetic analyses with
906 thousands of taxa and mixed models. *Bioinformatics* **22**, 2688–2690 (2006).
907 122. Felsenstein, J. A comparative method for both discrete and continuous characters using
908 the threshold model. *Am. Nat.* **179**, 145–56 (2012).
909 123. Revell, L. J. ANCESTRAL CHARACTER ESTIMATION UNDER THE THRESHOLD
910 MODEL FROM QUANTITATIVE GENETICS. *Evolution (N. Y.)*. **68**, 743–759 (2014).
911 124. Ihaka, R. & Gentleman, R. R: A Language for Data Analysis and Graphics. *J. Comput.*
912 *Graph. Stat.* **5**, 299–314 (1996).
913 125. Camacho, C. *et al.* BLAST+: Architecture and applications. *BMC Bioinformatics* **10**, 1–9
914 (2009).
915 126. Ohm, R. A. *et al.* Diverse Lifestyles and Strategies of Plant Pathogenesis Encoded in the
916 Genomes of Eighteen Dothideomycetes Fungi. *PLoS Pathog.* **8**, e1003037 (2012).
917 127. Katoh, K., Misawa, K., Kuma, K. & Miyata, T. MAFFT: a novel method for rapid multiple
918 sequence alignment based on fast Fourier transform. *Nucleic Acids Res.* **30**, 3059–66
919 (2002).
920 128. Stamatakis, A. RAxML version 8: A tool for phylogenetic analysis and post-analysis of
921 large phylogenies. *Bioinformatics* **30**, 1312–1313 (2014).
922 129. Chen, K., Durand, D. & Farach-Colton, M. NOTUNG: A Program for Dating Gene
923 Duplications and Optimizing Gene Family Trees. *J. Comput. Biol.* **7**, 429–447 (2000).
924 130. Nagy, L. G. *et al.* Comparative genomics of early-diverging mushroom-forming fungi
925 provides insights into the origins of lignocellulose decay capabilities. *Mol. Biol. Evol.* **33**,
926 959–970 (2016).
927 131. Park, G. *et al.* Global Analysis of Serine-Threonine Protein Kinase Genes in *Neurospora*
928 *crassa*. *Eukaryot. Cell* **10**, 1553–1564 (2011).
929 132. Nagy, L. G. *et al.* Genetic Bases of Fungal White Rot Wood Decay Predicted by
930 Phylogenomic Analysis of Correlated Gene-Phenotype Evolution. *Mol. Biol. Evol.* **34**, 35–
931 44 (2017).

932
933
934
935
936
937
938
939
940
941

942
943
944
945
946
947
948
949
950
951
952
953
954
955
956
957
958
959
960
961
962
963
964
965
966
967
968
969
970
971
972
973
974
975
976
977
978
979
980
981
982
983
984

Supplementary Figures

For

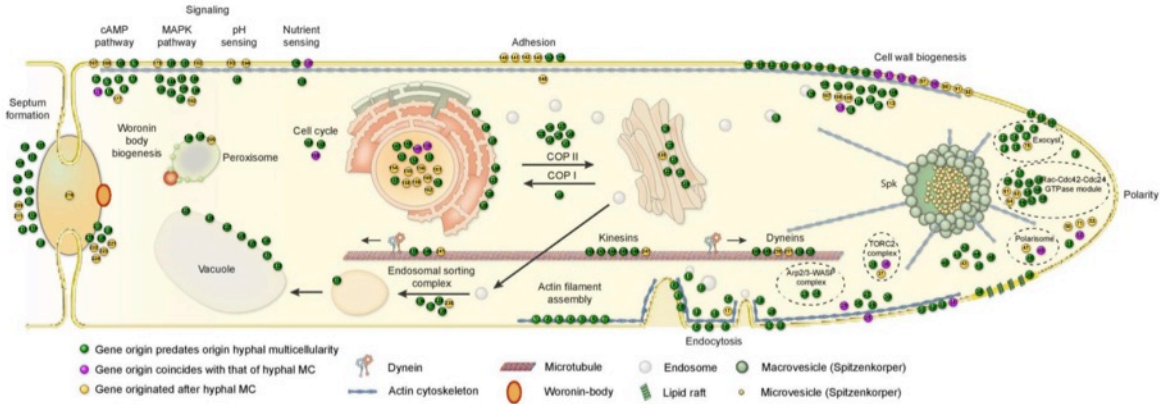
Comparative genomics reveals the origin of hyphae and multicellularity

Enikő Kiss, Botond Hegedüs, Torda Varga, Zsolt Merényi, Tamás Kószó, Balázs Bálint, Arun N. Prasanna, Meritxell Riquelme, Norio Takeshita, László G. Nagy

Contents:

- Supplementary Figure 1. Phylogenetic age distribution of hypha morphogenesis genes.*
- Supplementary Figure 2. Statistical comparisons of basic structural properties of genes related to hyphal MC.*
- Supplementary Figure 3. Reconstructions of ancestral gene copy numbers of histidine-kinase genes.*
- Supplementary Figure 4. Reconstructions of ancestral gene copy numbers of NADPH-oxidase genes.*

985



1 pfv1_Afu4g03050	51 Afu1g02920 (mesA in A.nidulans)	101 pld3_Afu3g05630	151 sebA_Afu4g09080	201 Afu6g02840
2 act1_Afu6g04740	52 Afu4g04120	102 Afu5g05550 (myov_myoE in A.nidulans)	152 MAT1-2_Afu3g06170	202 aspC_Afu5g03080
3 Afu1g10570 (coffin in A.nidulans)	53 Afu1g06090 (tearE in A.nidulans)	103 dbA_Afu2g06050	153 Afu3g06040	203 Afu1g02940
4 Afu1g03060	54 scm8_Afu2g13430	104 Afu2g01510	154 Afu2g05020 (dopa in A.nidulans)	204 aspB_Afu7g05370
5 Afu3g09350	55 chsE_Afu2g13440	105 Afu6g02920 (synA in A.nidulans)	155 Afu4g04502	205 Afu6g10330
6 Afu1g10060	56 hst1_Afu2g12400	106 Afu5g10810	156 Afu2g10770	206 aspA_Afu5g08540
7 Afu2g14270	57 Afu6g02810 (elmo_1ike in A.nidulans)	107 Afu2g07590	157 steA_Afu5g06190	207 aspE_Afu3g07015
8 Afu3g12080 (arfb in A.nidulans)	58 Afu2g05740 (modA in A.nidulans)	108 Afu5g05770	158 Afu2g12910	208 Afu5g02220
9 Afu4g10020	59 rcaA_Afu3g05300	109 Afu3g05580	159 Afu7g02260	209 Afu1g13170
10 Afu5g07930	60 rho1_Afu6g06900	110 Afu2g13760	160 ace2_Afu3g11250	210 Afu2g12390 (mobA in A.nidulans)
11 Afu4g08040 (ratB in A.nidulans)	61 Afu1g04340 (stock180_1ike in A.nidulans)	111 Afu6g02510	161 pacC_Afu3g11970	211 Afu6g05680
12 Afu2g02810	62 Afu2g11860	112 Afu1g12040	162 weta_Afu4g13230	212 Afu1g11010
13 Afu2g01200	63 Afu3g06280	113 ags2_Afu2g11270	163 Afu2g16840	213 cdcA_Afu3g12250
14 Afu6g02070 (infA in A.nidulans)	64 Afu5g07430	114 Afu3g12800	164 Afu4g12160	214 Afu5g08700 (myoB in A.nidulans)
15 Afu7g03680	65 rho4_Afu2g14060	115 Afu6g02320	165 Afu6g04810	215 hysA_Afu3g14480
16 sac6_Afu2g07420	66 Afu2g15050	116 gfa1_Afu6g06340	166 Afu4g06130	216 Afu6g06520
17 Afu2g10220	67 Afu4g14450 (cdc24 in A.nidulans)	117 Afu5g06670	167 gpcC_Afu2g12640	217 Afu7g05950
18 Afu2g08850 (dnfB in A.nidulans)	68 Afu5g11380	118 Afu1g10970	168 gpcC_Afu7g04800	218 Afu5g03940
19 Afu6g02850	69 rsm2_Afu5g08550	119 Afu6g04840 (hysA in A.nidulans)	169 gprI_Afu3g00780	219 casI_Afu5g09360
20 Afu6g02540	70 rcaA_Afu1g11230	120 Afu5g03580 (gpp8B in A.nidulans)	170 gprC_Afu3g01150	220 cnbB_Afu4g04540
21 Afu5g05950	71 Afu2g02520 (teea in A.nidulans)	121 Afu4g10040	171 staD_Afu5g12210	221 Afu5g03400
22 Afu3g14230	72 Afu6g11370 (exoB4 in A.nidulans)	122 kevB_Afu4g12970	172 gpaA_Afu1g13140	222 ENO1_Afu1g04260
23 Afu1g13330 (arp2)	73 Afu1g13790 (cecE in A.nidulans)	123 Afu5g11960	173 gpaB_Afu1g12930	223 bud4_Afu2g06470
24 Afu6g05660 (myoA in A.nidulans)	74 Afu6g02790	124 Afu4g08850	174 Afu1g13250	224 Afu5g11890 (bud3 in A.nidulans)
25 Afu7g03870	75 Afu2g11960 (exo70 in A.nidulans)	125 Afu6g03840	175 rcaA_Afu4g08820	225 Afu1g04080 (vps52 in A.nidulans)
26 Afu1g05930	76 Afu6g02590 (cec15 in A.nidulans)	126 Afu6g07290	176 rcaA_Afu6g08320	226 Afu4g07110
27 pti1_Afu6g07520	77 Afu4g10490 (cecE in A.nidulans)	127 Afu1g11470	177 pdeB_Afu1g05230	227 Afu5g13540
28 Afu3g06140 (slbB in A.nidulans)	78 Afu1g04350 (cecC in A.nidulans)	128 Afu3g08840 (copA in A.nidulans)	178 pkaR_Afu3g10000	228 Afu1g05280 (vps8 in A.nidulans)
29 Afu6g04520	79 Afu5g08040 (cecE in A.nidulans)	129 Afu4g07390	179 pkaE_Afu5g07980	229 Afu6g04870 (vps45 in A.nidulans)
30 Afu1g13020	80 ger1_Afu6g12410	130 Afu3g09700	180 sho1_Afu5g08420	230 Afu5g02360 (vpsA in A.nidulans)
31 Afu4g03160	81 crk3_Afu3g09250	131 Afu4g13150	181 Afu3g09740	231 Afu1g10810
32 Afu5g05710 (swcC in A.nidulans)	82 ccm3_Afu4g06820	132 hysB_Afu7g05700	182 preB_Afu3g13330	232 Afu2g13750 (hbrA in A.nidulans)
33 Afu1g02900	83 kn6_Afu2g11870	133 pm2_Afu1g07690	183 sak1_Afu5g08390	233 Afu2g04740 (vps27 in A.nidulans)
34 rpbB_Afu4g12640	84 chsA_Afu3g03760	134 pm4_Afu6g04500	184 sakB_Afu1g10940	234 Afu1g02220 (vps20 in A.nidulans)
35 Afu2g10460	85 Afu4g06620	135 Afu2g12580	185 ptcG_Afu5g13340	235 Afu3g13890 (vps24 in A.nidulans)
36 Afu6g07910	86 chsA_Afu2g01870	136 Afu2g02340	186 Afu5g06420	236 Afu3g14380 (vps23 in A.nidulans)
37 sm1_Afu2g12210	87 chsB_Afu4g01880	137 Afu5g13210	187 sakA_Afu1g12340	237 Afu1g04200 (vps33 in A.nidulans)
38 Afu3g13440 (staA in A.nidulans)	88 chC_Afu5g00760	138 chw11_Afu6g04210	188 mpkB_Afu6g12820	238 Afu4g04100
39 Afu4g06290 (bnaA in A.nidulans)	89 chg_Afu3g14420	139 Afu1g05470	189 artA_Afu2g03290	239 Afu1g13390 (mpkA in A.nidulans)
40 steA_Afu7g03760	90 scm4_Afu6g12380	140 roaA_Afu5g09580	190 sak_Afu6g11470	240 epi_Afu3g11860
41 Afu3g06080	91 crmA_Afu6g14090	141 rodB_Afu1g17250	191 vpd1_Afu4g10280	241 Afu2g08190 (coa in A.nidulans)
42 Afu2g02530	92 ags1_Afu3g00910	142 rodE_Afu6g05090	192 Afu4g04070	242 Afu2g03150
43 Afu2g08180 (fbaA in A.nidulans)	93 exo1_Afu1g03600	143 gtrB_Afu3g12700	193 Afu3g14900	243 Afu7g01460
44 erg9_Afu7g01220	94 chs3_Afu8g05620	144 Afu2g12180	194 path_Afu5g13270	244 Afu6g04660 (c1pA in A.nidulans)
45 Afu4g08070 (swdF in A.nidulans)	95 lgl1_Afu1g11460	145 Afu1g01540	195 Afu6g04600	245 Afu1g14220
46 Afu6g12920	96 neq1_Afu6g07120	146 gpaA_Afu3g02970	196 meaa_Afu2g05880	246 Afu3g14730
47 Afu1g09940	97 swm1_Afu7g05450	147 Afu8g05570	197 Afu2g08800	247 Afu7g03710 (k1pA in A.nidulans)
48 Afu2g03710 (sepA in A.nidulans)	98 chn2_Afu1g12600	148 hst1_Afu5g01300	198 pen11_Afu6g07740	248 Afu3g10720
49 Afu6g04940 (sepA in A.nidulans)	99 chsF_Afu8g05630	149 stuA_Afu2g07900	199 Afu2g17000 (wscA in A.nidulans)	249 Afu2g13450 (nudM in A.nidulans)
50 Afu1g11920 (teac in A.nidulans)	100 otrA_Afu3g05650	150 medA_Afu2g13260	200 hexA_Afu5g08830	250 Afu5g08430

986

987

988 Supplemental Figure 1. Phylogenetic age distribution of hypha morphogenesis genes. Figure
989 mirrors main text Figure 2 with gene names provided for each dot.

990

991

992

993

994

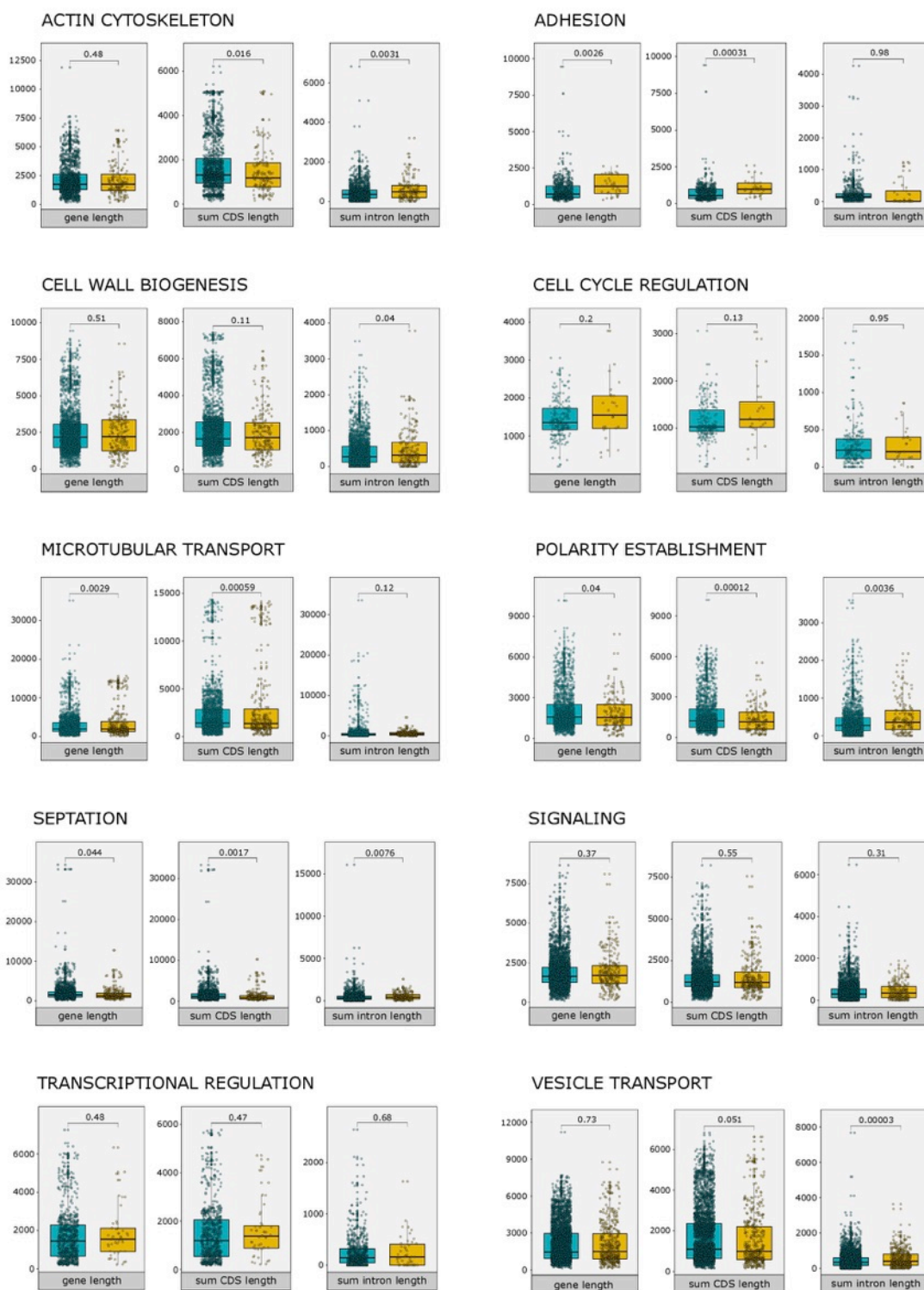
995

996

997

998

999

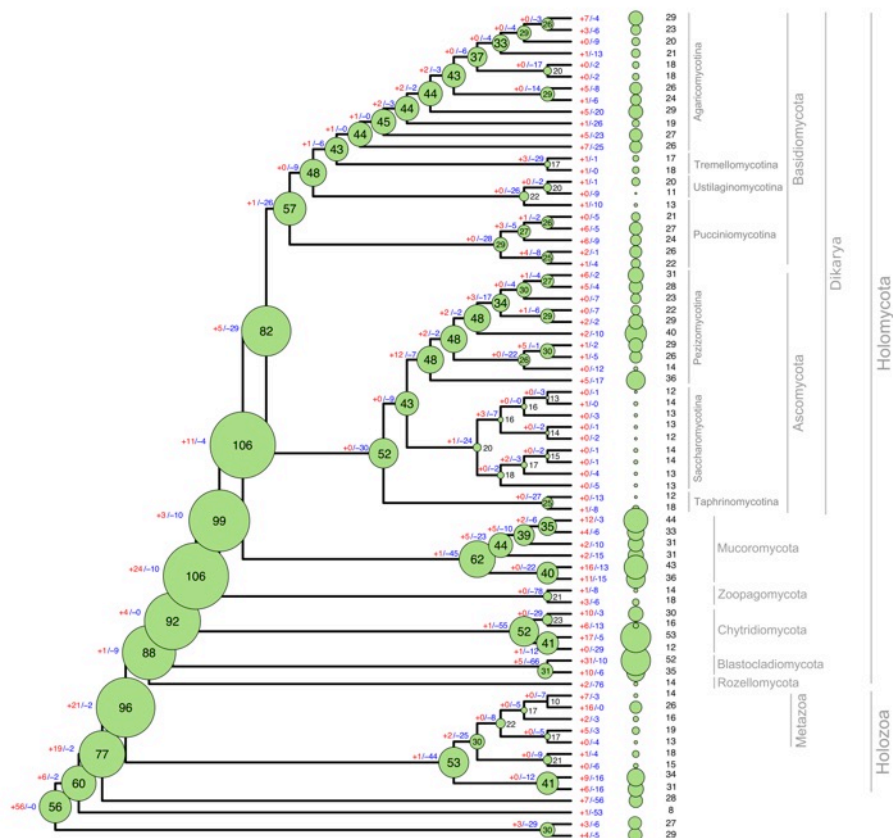


1000

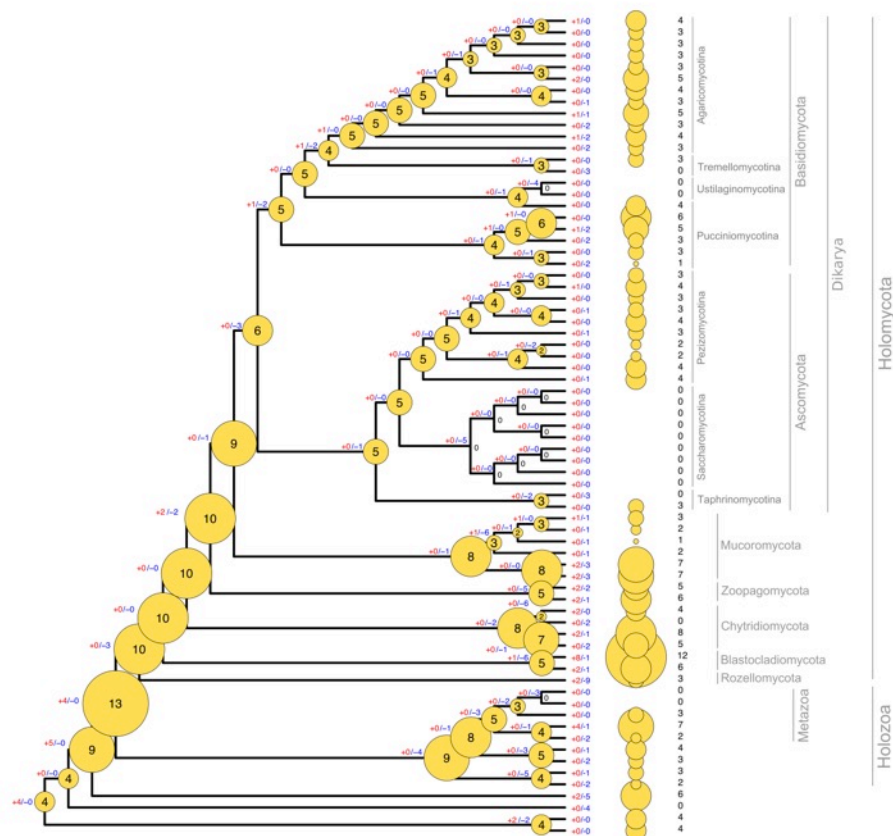
 multicellular fungi

 unicellular fungi

1001 Supplementary Figure 2. Statistical comparisons of basic structural properties of genes related
1002 to hyphal MC. Box plots display differences in gene, CDS and intron lengths of 4 unicellular
1003 (yellow) and 39 multicellular fungi (blue) in nine functional categories.
1004



1005
1006 Supplementary Figure 3. Reconstructions of ancestral gene copy numbers of histidine-kinase
1007 genes. Numbers at the branches represent gene duplications (+) and losses (-) inferred by
1008 COMPARE. Bubble size is proportional to reconstructed ancestral gene copy number. Copy
1009 number distribution for each species is shown right to the tree.
1010
1011
1012
1013
1014
1015
1016
1017
1018
1019
1020
1021
1022



1023
1024 Supplementary Fig. 4. Reconstructions of ancestral gene copy numbers of NADPH-oxidase
1025 genes. Numbers at the branches represent gene duplications (+) and losses (-) inferred by
1026 COMPARE. Bubble size is proportional to reconstructed ancestral gene copy number. Copy
1027 number distribution for each species is shown right to the tree.
1028
1029